

Conversion of a Gas Turbine Engine to Operate on Lean-Premixed Hydrogen-Air: Design and Characterization

Jordan Thomas Farina

Thesis submitted to the faculty of the
Virginia Polytechnic Institute and State University
in partial fulfillment of the requirements for the degree of

Master of Science
In
Mechanical Engineering

Uri Vandsburger, Chair
Walter F. O'Brien
Stephen D. LePera

Jan. 18, 2010
Blacksburg, Virginia

Keywords: Hydrogen, Lean-Premixed, Gas Turbine

Conversion of a Gas Turbine Engine to Operate on Lean-Premixed Hydrogen-Air: Design and Characterization

Jordan Thomas Farina

ABSTRACT

The continued use of fossil fuels along with a rise in energy demand has led to increasing levels of carbon emissions over the past years. The purpose of this research was to design a lean premixed hydrogen fuel system that could be readily retrofit into an existing gas turbine engine to provide a clean renewable energy solution to this growing problem. There were major hurdles that had to be overcome to develop a hydrogen fuel system that would be practical, stable, and would fit into the existing space.

High flame temperatures coupled with high flame speeds are major concerns when switching from jet fuel or natural gas to hydrogen. High temperatures lead to formations of pollutants such as oxides of nitrogen (NO_x) and can potentially cause damage to critical engine components. High flame speeds can lead to dangerous flashbacks in the fuel premixers. Past researches have developed various hydrogen premixers to combat these problems. This research designed and developed new hydrogen premixers using information gathered from these designs and utilized new ideas to address their shortcomings.

A gas turbine engine was modified using 14 premixers and a matching combustor liner to provide lean operation with the existing turbomachinery. The engine was successfully operated using hydrogen while maintaining normal internal temperatures and practically eliminating the NO_x emissions when compared to normal Jet-A operation. Even though full power operation was never achieved due to flashbacks in two premixers, this research demonstrated the feasibility of using lean-premixed hydrogen in gas turbine engines.

Acknowledgements

I would like to thank Bruce Cambata and Joe Garst of Electric Jet LLC. for funding this project. Without their vision and support, I would not have had the opportunity to work on a project that I believe, along with them, is such an important issue. Also, I would like to thank Steve LePera, Matt Perry, Dan Villarreal, David Sykes, and Bill Hook. Without all of these people, this project would have never achieved so much. I would also like to thank Dr. Uri Vandsburger and Dr. Walter F. O'Brien for allowing me the opportunity to work on this project, and providing useful insight and guidance throughout. I would also like to thank Joe Ranalli for donating his time and expertise to helping this project.

I would also like to thank my mom and dad for helping throughout my educational career and through life in general. They were both there for me through any situation that ever arose, and I always knew I could count on them.

I would also like to thank all of the friends that I have made through my many years in school. They are the ones that made this time great.

Table of Contents

ABSTRACT.....	ii
Acknowledgements.....	iii
Table of Contents.....	iv
List of Figures.....	vi
List of Tables.....	ix
Chapter 1: Introduction.....	1
1.1 Motivation.....	1
1.2 Background.....	2
1.2.1 NO _x Formation.....	2
1.2.2 NO _x Control Strategies.....	3
1.2.3 H ₂ Enrichment on Lean Premixed Systems.....	5
1.2.4 Stability of Lean Premixed.....	5
1.2.5 Flame Speed and Internal Velocity of the Premixer.....	6
1.2.6 Stabilization.....	8
1.2.7 Mixing.....	10
1.2.8 Engine.....	12
Chapter 2: Project Goals.....	13
2.1 Objectives and Expectations.....	15
2.1.1 Lean Hydrogen Premixer.....	15
2.1.2 Combustor Liner.....	15
2.1.3 Engine.....	15
2.2 Thesis Outline.....	16
Chapter 3: Premixer.....	17
3.1 Collecting Engine Data.....	17
3.2 Premixer Design.....	18
3.3 Computational Set-Up.....	26
3.4 Computational Results.....	29
3.5 Prototype Manufacturing.....	30
3.6 Experimental Set-Up.....	32
3.7 Experimental Tests and Results.....	36

3.8 Discussion	39
Chapter 4: Combustor Liner	43
4.1 Combustor Liner Design.....	43
4.2 Testing of Combustor Liner Section with Premixer	48
4.3 Combustor Liner Manufacturing	51
4.4 Discussion	53
Chapter 5: Lean Premixed Hydrogen Engine.....	56
5.1 Engine Set-up.....	56
5.2 Engine Testing and Results.....	58
5.3 Discussion.....	59
Chapter 6: Summary and Recommendations for Future Work	62
6.1 Summary	62
6.2 Recommendations for Future Work.....	63
References.....	68
Appendix A: Premixer Drawings	71
Appendix B: Computational Model	75
Appendix C: Combustor Drawings	76

List of Figures

Figure 1.1 Carbon dioxide emissions in the United States from 1990 to 2007. www.eia.doe.gov	1
.....	
Figure 1.2. NO and N ₂ O formation using PSR model.	4
Figure 1.3. Flame temperature using PSR model.	4
Figure 1.4. Increase in inner turbine temperature with increase in combustor pressure drop.	8
Figure 1.5. Schematic showing a swirl stabilized premixer.	9
Figure 1.6. Illustration showing how introducing the hydrogen into wakes or high turbulence regions promote flashback.	11
Figure 2.1. Schematic of a Jet_A fueled gas turbine engine.	14
Figure 2.2. Schematic of a lean premixed hydrogen fueled gas turbine engine.	14
Figure 3.1. Compressor outlet temperature and pressure versus engine power level.	18
Figure 3.2. Air and energy equivalent hydrogen flow rates versus engine power.	18
Figure 3.3. Section View of Premixer Concept.	20
Figure 3.4. 3-D CAD models of the premixer: (left) isometric view (right) downstream exit view	21
.....	
Figure 3.5. 3-D CAD models of the centerbody with vanes.	22
Figure 3.6. Contour plot of velocity magnitude in X-Z direction at the hydrogen injection plane at the full power condition. The wakes and location of fuel ports are illustrated.	25
Figure 3.7. 2-D section of volume mesh, along with mesh of the hydrogen injection plane.	27
Figure 3.8. Contours of equivalence ratio at the exit of the premixer under idle engine conditions.	30
Figure 3.9. Disassembled Premixer. Photo by author, 2009.	31
Figure 3.10. Assembled Premixer. Photo by author, 2009.	32
Figure 3.11. Configurations that can be tested: a.) single premixer, b.) three side by side premixers, and c.) premixer with liner section. Flow travels from left to right.	32
Figure 3.12. Facility at the CSDL.	33
Figure 3.13. Assembled test section. Flow travels from left to right. The fuel line (not shown) would pass through a fitting and attach to the premixer.	34
Figure 3.14. Exploded view of test section. The configuration shown is for the single premixer set-up.	34

Figure 3.15. Assembled test combustor at CSDL. Photo by Dan Villarreal, 2009, used with permission.	35
Figure 3.16. Test combustor enclosed in pressure shell to allow for high pressure testing at CSDL. Photo by author, 2009.	36
Figure 3.17. Picture of flame during operation. . Photo by author, 2009.	38
Figure 3.18. Shows the test set up to measure the discharge coefficients. Rig was used measure discharge coefficients for the premixer and for dilution and cooling holes in the liner.	38
Figure 3.19. Discharge coefficient for premixer. Constant at 0.8 for all relevant flow conditions.	39
Figure 3.20. Picture of flame looking down the premixer. The five rich zones that were predicted by the CFD are easily distinguishable. Photo by author, 2010.	40
Figure 4.1. Original combustor liner for the PT6 turboprop engine using Jet-A fuel. Photos by Dan Villarreal, 2009, used with permission.	44
Figure 4.2. (a) Splash ring style, (b) double splash ring style cooling holes.	45
Figure 4.3. Air flow split showing total air produced by compressor, air flow required for premixer operation (59%), and air flow through combustor liner (41%). Percentage is in reference to total air flow.	46
Figure 4.4. Predicted premixer internal air and mixture velocities with corresponding pressure drop across the premixer, all versus power level.	48
Figure 4.5. Predicted equivalence ratio.	48
Figure 4.6. Schematic and picture of test set-up. Photo by author, 2009.	49
Figure 4.7. Flame picture along the actual operating line. (1) 38hp 0.33 eq ratio (2) 190hp 0.29 eq ratio (3) 365hp 0.34 eq ratio. These 3 conditions give a good representation of flame structure at low, medium, and high power conditions, respectively. Photos by author, 2009.	50
Figure 4.8. Inconel liner plate designed to hold 14 premixers, 4 igniters, and 119 unblocked dilution holes.	52
Figure 4.9. Picture showing the welded plugs and weld holding the liner plate. Photo by author, 2009.	52
Figure 4.10. Lean premixed hydrogen combustor liner. Photos by author, 2009.	53
Figure 4.11. Example of staged acceleration.	54

Figure 5.1. Lean premixed hydrogen combustor; consists of 14 hydrogen premixers, a combustor liner, and 4 igniters. Photo by author, 2009.	57
Figure 5.2. PT6A-20 up-fitted with lean premixed hydrogen combustor. Photo by author, 2009.	57
Figure 5.3. Comparison of NO _x formation between the original Jet-A engine, the previous iteration of lean premixed hydrogen, and the most recent lean premixed hydrogen combustor design.	59
Figure 5.4. Comparison of inner turbine temperatures (T5) between the original Jet-A engine, the previous iteration of lean premixed hydrogen, and the most recent lean premixed hydrogen combustor design.	59
Figure 6.1. Set-up used to capture combustion instabilities.	65
Figure 6.2. Power spectrum for PMT measurements. Peaks at 450Hz and 1200 Hz represent the instabilities.	66
Figure 6.3. Phased averaged images over 1 period. Each picture was averaged at every 45 degrees of phase. Photos by Joe Ranalli, 2009, used with permission.	67
Figure A.1. TOP, FRONT, and ISO view of Premixer.....	71
Figure A.2. Section view of Premixer.	72
Figure A.3. FRONT, ISO, and RIGHT view of Centerbody.....	72
Figure A.4. TOP, FRONT, and ISO view of Premixer Shell.....	73
Figure A.5. TOP, FRONT, and ISO view of Fuel Manifold Casing.....	74
Figure C.1. FRONT, BACK, ISO, and RIGHT view of Front Combustor Plate.....	76
Figure C.2. FRONT, BACK, ISO, and RIGHT view of Back Combustor Plate.....	77
Figure C.3. TOP, FRONT, and ISO view of Combustor Window Cover.....	78
Figure C.4. TOP, FRONT, and ISO view of Liner Section used for Testing.....	78

List of Tables

Table 3.1. Engine conditions and constraints on the cross sectional area of each pre-mixer.	21
Table 3.2. Boundary conditions used in the air only simulations under idle and full power engine conditions.....	28
Table 3.3. Boundary conditions used for the hydrogen/air simulation under idle conditions.	28
Table 3.4. Test matrix for static stability test at low engine power level conditions.....	37
Table 4.1. Discharge coefficients for the pre-mixer, 6 rows of splash ring cooling holes, and 3 standard sizes.	45
Table 4.2. Test conditions and stability results for the liner section with the pre-mixer.	50
Table 6.1. Comparison of design parameters for the pre-mixer to the restrictions and constraints placed on the design.....	62
Table B.1. Settings used for the Computational Model.....	75

Chapter 1: Introduction

This chapter provides information on multiple topics that are important in the design of a lean premixed hydrogen-air fueled gas turbine engine and the motivations for pursuing this technology. Section 1.1 illustrates the need for clean renewable energy systems and how hydrogen can meet this need. Section 1.2 provides information to address the unique set of challenges that arise when using hydrogen as the fuel. This section discusses fundamentals of hydrogen combustion as well as restrictions and constraints on the design of the hydrogen combustor, including those imposed by the engine chosen for modification. This engine was a Pratt and Whitney PT6A-20 turboprop engine.

1.1 Motivation

The continued use of fossil fuels along with a rise in energy demand has led to increasing levels of carbon emissions over the past years.¹ The elevated levels of greenhouse gases produced from power generation and transportation has led to a growing concern over global climate conditions. As of 2007, only about 8% of the energy produced in the United States came from renewable sources.

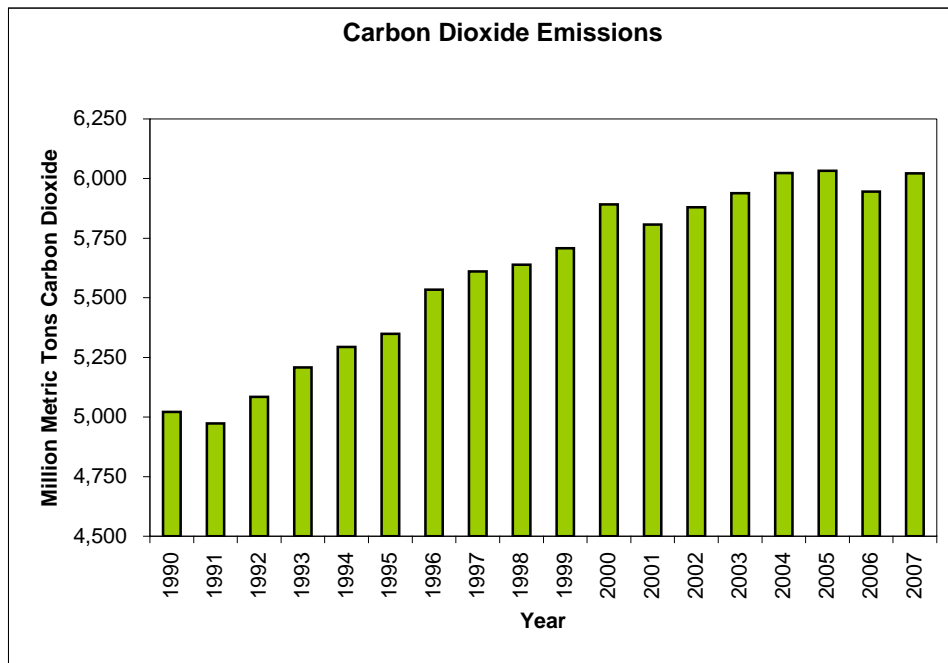


Figure 1.1 Carbon dioxide emissions in the United States from 1990 to 2007. www.eia.doe.gov

Hydrogen provides a carbon free energy solution, and, if used correctly, can eliminate other harmful emissions such as Oxides of Nitrogen (NO_x). Hydrogen can be produced in a variety of

ways, the cleanest of which is the electrolysis of water. However, this process requires an extremely large amount of energy. The energy can come from clean renewable sources such as wind, solar, hydroelectric, or even nuclear power, thus eliminating all carbon emissions. The hydrogen can then be used to fuel the growing energy demand and release our country from the need for foreign oil.

Hydrogen has been used experimentally in some of the earliest gas turbine engines where it was burned in pure diffusion mode.² Unfortunately, the burning of fuel in a diffusion flame causes very high flame temperatures, particularly with hydrogen. As will be discussed in detail later, NO_x generation increases exponentially with temperature and thus diffusion flames typically produce large quantities of these pollutants. In 2005, Chiesa et al.³ investigated the effects of operating large-scale natural gas fueled gas turbines on hydrogen to help reduce greenhouse emissions. The computational study showed that small decreases in efficiency occurred because of either the redesign of components or the use of NO_x control strategies. However, this study did not include operating the engine using a lean premixed combustor because it was thought to be a “questionable practice” due to the nature of hydrogen.

This project attempted to develop new lean premixed hydrogen combustors for existing gas turbines. Lean premixed hydrogen-fueled engines would not only reduce greenhouse emissions, but also oxides of nitrogen, while suffering no loss in performance compared to engines operating on conventional fossil fuels.⁴

1.2 Background

1.2.1 NO_x Formation

There are three main chemical mechanisms or pathways in which NO_x is created in combustion. The first and most dominant is the thermal or Zeldovich mechanism. The main contributors to the formation of NO_x in this mechanism are flame temperature and residence time.⁵⁻⁶ Thermal NO_x only forms at high temperatures in the post flame zone due to the slow reaction rates of this mechanism. At a flame temperature around 1800 K, the production rate of NO_x increases rapidly. At lower temperatures, however, NO_x formation is minimal, even for longer residence times. Either operating the combustor at lower temperatures or rapidly diluting the hot gases to “freeze” the reaction before it can have a chance to form can control thermal NO_x. These high flame temperatures can be avoided by operating the combustors at lean equivalence ratios. However, these lean, low temperature conditions promote the formation of

NO_x through the second mechanism, the N₂O-Intermediate mechanism. The formation through this mechanism is important but small in comparison to thermal NO_x production. The third contributor to NO_x formation in hydrocarbon systems is the prompt NO as described by the Fenimore mechanism. This NO is formed in the flame zone long before enough time has passed for the creation of thermal NO. However, this reaction requires the presence of carbon to bond with molecular nitrogen to form amines or cyano compounds that later convert to form NO.⁵⁻⁶ Hydrogen is an ideal fuel for NO_x reduction because it does not have a carbon bond and can operate at extremely lean conditions due to its high flame speed and high extinction strain rates.

1.2.2 NO_x Control Strategies

There are various ways to remove or prevent NO_x in gas turbine engines. One method is to cool the flame zone by introducing another medium to absorb the energy, thus lowering the temperature and decreasing the formation of thermal NO_x. This can be performed by injecting steam, water, or nitrogen, or by the recirculation of exhaust gases back into the combustion zone. However, all of these methods require additional components to inject the medium into the system. In the case of nitrogen injection, an additional air separator would be required to obtain the nitrogen from the atmosphere. Another method is post combustion treatment of the exhaust gases. Many of these techniques involve the injection of ammonia into the hot exhaust gases to reduce NO to N₂. These systems can be very expensive to install and operate. The most attractive option to reduce NO_x is by using a lean premixed combustor. Lean premixed combustors, also known as dry low NO_x combustors, mix the fuel with an excessive amount of air upstream of the flame zone to achieve a lower temperature flame zone. The fundamental idea is similar to the steam/water/nitrogen injection, but this technique requires no additional systems to be added to the combustor. Homitz⁷ reviews the state of the art technology in dry low NO_x burners.

Equivalence ratio is the main driving factor for the flame temperature and also the formation of NO_x. A perfectly stirred reactor (PSR) model was created, using *CHEMKIN*,⁸ to estimate the flame temperature and NO_x production at a range of equivalence ratios. The model was based on the approximate volume the flame will inhabit inside of the combustor in the engine. Also, the inlet conditions were based on the full power compressor outlet conditions of the PT6 engine. The residence time was allowed to vary based on the mass flow and flame temperature inside of

the volume. The data in Figure 1.2 and Figure 1.3 show the flame temperature as well NO and N₂O formation as a function of equivalence ratio. It is clear that below an equivalence ratio of about 0.5 the formation of NO very small.

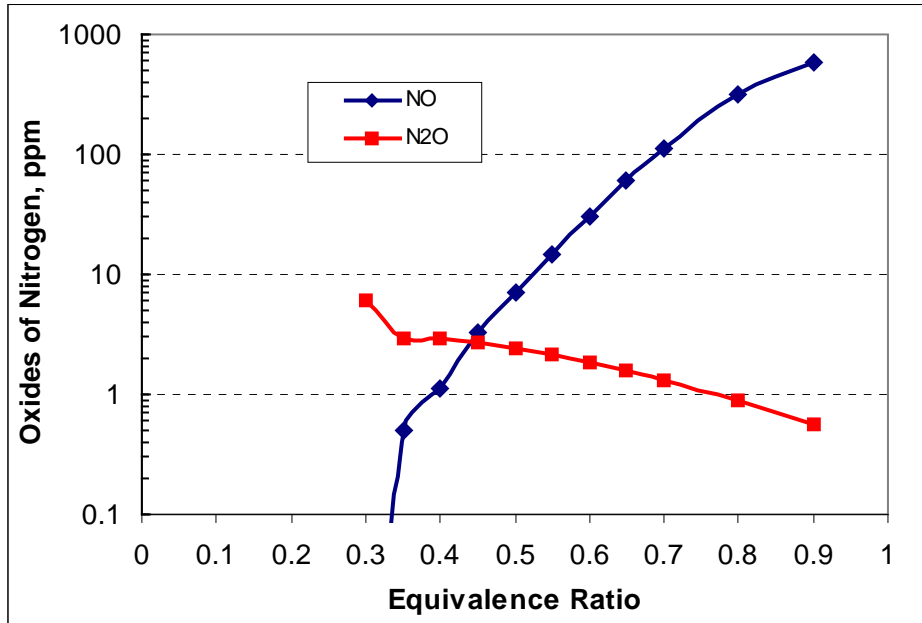


Figure 1.2. NO and N₂O formation using PSR model.

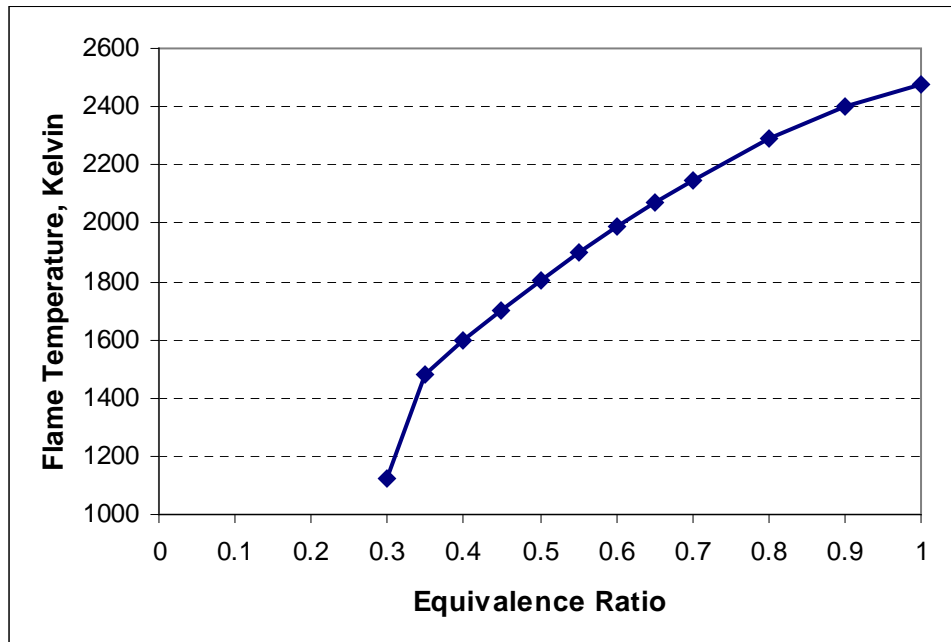


Figure 1.3. Flame temperature using PSR model.

1.2.3 H₂ Enrichment on Lean Premixed Systems

In typical gas turbines operated on lean premixed hydrocarbon fuels, there is a limit on how lean the combustor can operate. If operated too lean, the burners cannot sustain combustion or they suffer from a lack of efficiency. At these lean conditions, the low flame temperature along with the high strain rates lead to incomplete combustion. This leads to a high concentration of CO and unburned hydrocarbons (HC) in the exhaust. Many researchers have shown that simply adding H₂ can improve the lean stability of hydrocarbon fuels thus allowing for leaner and lower NO_x combustion.⁹⁻¹⁴ In these studies, hydrogen was added to the hydrocarbon fuel, typically methane, and compared to the flame without hydrogen. The researchers observed more compact and robust flame zones with enhanced lean stability. Researchers suggested that the presence of hydrogen increases the rate at which the radical pools, composed of O, OH, and H radicals, are formed in the flame zone. The radicals increase the rates of many reactions allowing for faster, more complete combustion. This allows for overall leaner mixtures, producing lower NO_x, while suffering no loss in combustor efficiency due to incomplete combustion.

1.2.4 Stability of Lean Premixed

Lean premixed flames are susceptible to problems with stability. Past research has shown that lean premixed systems, when operated near the flammability limit, can experience various instabilities.^{9, 14} Stability can be classified in two ways: dynamic and static, even though in many cases the dynamics of the flame can affect the static stability. Static stability focuses on two major issues, flashback and blowoff. Blowoff occurs when there is a lack of energy transfer to the unburned gases from the hot products necessary to sustain combustion.⁶ Flashback occurs when the flame propagates upstream into the mixing zone. Due to the high flame speed and reactivity of hydrogen, flashback is a much more serious issue than blowoff. Dynamic stability refers to how pressure and velocity perturbations caused by combustion can lead to fluctuations in equivalence ratio and heat release that can potentially cause the system to go unstable. This research currently addresses static stability, acknowledging that future research should investigate dynamic stability. Both Tuncer¹⁴ and Ghoniem⁹ have provided some insight into the stability effects of adding hydrogen to a combustion system.

There are four main mechanisms that cause flashbacks in premixing combustors: 1) flame propagation into the boundary layer, 2) turbulent flame speed exceeding the average upstream velocity, 3) combustion instabilities, and 4) combustion induced vortex breakdown.¹⁵⁻¹⁷ The first

mechanism most commonly appears in low velocity systems because the turbulent boundary layer in a high velocity system is very thin with a very strong velocity gradient preventing the flame from propagating. The turbulent flame speed of the mixture has a strong dependence on the equivalence ratio, temperature, pressure, and turbulence levels. As each of these parameters increase, so does the speed at which the flame can propagate. Combustion instabilities can cause fluxes in heat release that can alter the flame shape and size due to varying local mixture properties. This can cause velocity perturbations that can lead to momentary instances of reversed flow fields, allowing the flame to propagate upstream. Combustion induced vortex breakdown occurs when the flame changes or breaks down the recirculation zone where the flame is stabilized. This is common in premixers that utilize a fluid dynamically stabilized flame zone, such as a swirl combustor without a center body.

Lewis and von Elbe were among the first researchers to study flame flashback and were able to characterize the critical conditions at which laminar flames propagate upstream.¹⁸ Much research has been performed since these early studies on both laminar and turbulent flames, but it is still extremely difficult to predict flashback for a complex flow field. Plee and Mellor¹⁷ performed extensive research on a number of combustion systems in an effort to add insight into the conditions that promote flashback. The information gathered and studied by Plee and Mellor¹⁷ along with others greatly influenced the design of the premixers.

1.2.5 Flame Speed and Internal Velocity of the Premixer

The internal velocity of the premixer must exceed the turbulent flame speed of the lean hydrogen-air mixture to prevent flashbacks. The internal velocity was estimated using two factors, cross sectional area of the premixer and equivalence ratio. The equivalence ratio sets the air to fuel ratio. With the additional knowledge of the energy equivalent hydrogen fuel flow rate and the number of premixers needed, the mass flow through each premixer was set. This information was then used to size the premixer based on the desired internal velocity. More information on the sizing of the premixer is presented in section 3.2 Premixer Design.

Turbulent flame speeds of hydrogen mixtures were estimated using turbulent flame speed calculations and observations made by previous researchers. Plee and Mellor¹⁷ studied many different combustors and found flashback velocities to be between 15-18m/s for hydrogen mixtures at temperatures between 500-600 K and pressures between 3.8-5.2 atm. Also, using

flame speed correlations proposed by Damkohler⁵⁻⁶, with reference laminar flame speeds calculated by Kitagawa¹⁹ and an estimated turbulent intensity of 10%, flame speeds were estimated between 10-15m/s for simulated engine temperatures and pressures along with equivalence ratios between 0.4 and 1. Other correlations, such as the Kilmov model, estimate the flame speed to be between 15-30m/s for increasing equivalence ratios from 0.4-1.⁵⁻⁶ However, this model only claims to be valid for extremely high turbulence. Even though the engine is assumed to have lower turbulence, the internal constraint must be based on worst-case scenarios. Koroll et al.²⁰ measured the turbulent burning velocities of hydrogen air mixtures directly using a double-kernel technique. They found the same increasing trend as the other models: when the equivalence ratio (between 0.4 and 1) and turbulence level increases, so does the turbulent burning velocity of the mixture. This research found burning velocities up to about 25m/s, with relatively low turbulence levels compared to what is expected in our engine

Due to the complexity of predicting the conditions at which a flashback will occur, experimental work was performed on previous hydrogen premixers developed at Virginia Tech in an attempt to map out conditions at which flashbacks occurred. Perry²¹ presented this work in his Masters Thesis at Virginia Tech. In this work, flashback velocities in hydrogen premixers at engine operating temperatures and pressure were found as high as 80m/s at elevated equivalence ratios.

The design internal velocity of the pre-mixer must exceed the turbulent flame speed of the mixture. However, due to the characteristics of the turbomachinery, pressure drop across the pre-mixer is the constraining parameter when designing for an internal velocity. Previous iterations of hydrogen premixers developed at Virginia Tech used the extremely high velocity of 240m/s to prevent flashback, yet this was not an elegant solution.²¹ By designing for such a high internal velocity, it is impossible to also have a low-pressure drop combustor, and as shown Figure 1.4 increasing the pressure drop of the combustor above the original specifications causes an increase in Inner Turbine Temperature (ITT) due to decreased airflow. Since the decrease in airflow was not anticipated, the pre-mixer could not sustain the high internal velocity at which it was designed for and ultimately suffered flashbacks. From these results, it is clear that the hydrogen pre-mixer must be designed for a much lower pressure drop to avoid this situation. However, to decrease the pressure drop, the internal velocity must be lowered, yet not so low as to allow for the flame propagation due to the turbulent flame speed exceeding the axial velocity.

For this project, it was concluded that bulk flow internal axial velocities in the range of 70-100m/s should be adequate to prevent flashback without causing excessive pressure losses.

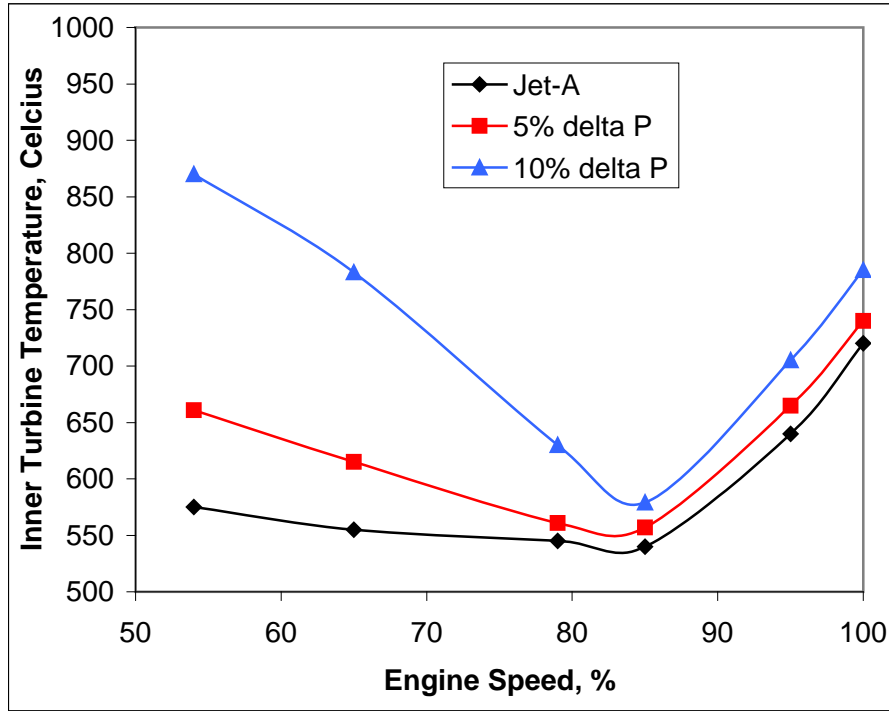


Figure 1.4. Increase in inner turbine temperature with increase in combustor pressure drop.

1.2.6 Stabilization

In addition to avoiding flashback, premer designs must provide adequate flame stabilization to prevent blowoff at low equivalence ratios. Swirl and dump plane stabilization are commonly used in lean premixed systems to anchor the flame at the exit of the premer, as shown in Figure 1.5.

The swirling flow creates a vortex breakdown in the core flow, which creates a recirculation zone that allows the hot products to transfer energy to the unburned gases.²² The degree of swirl is defined by a non-dimensional swirl number, S , that is defined as the ratio of the axial flux of angular momentum to axial flux of axial momentum, shown in Eq. 1.

$$S = \frac{\int U_x U_\theta r^2 dr}{r \int U_x^2 r dr} \quad (1)$$

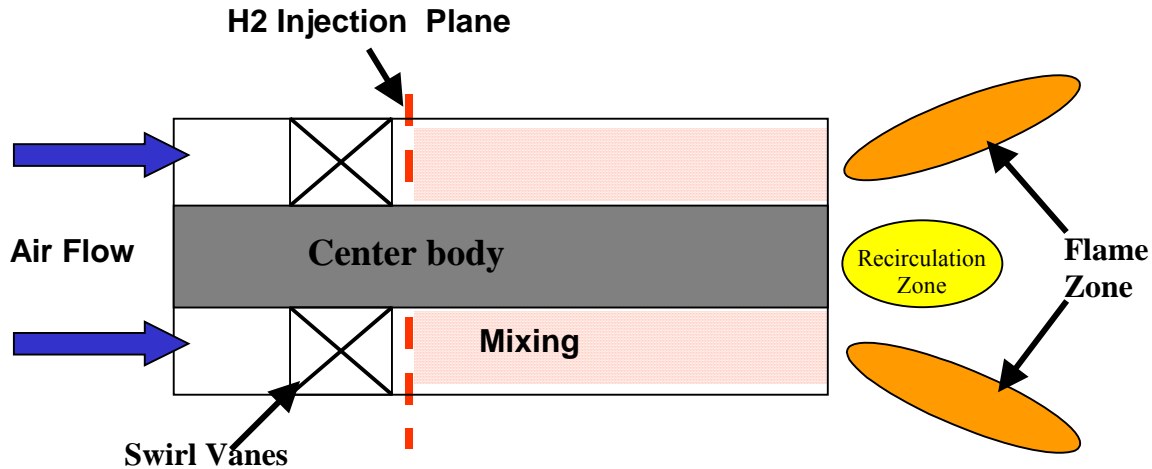


Figure 1.5. Schematic showing a swirl stabilized premixer.

Gupta's²³ book "Swirl Flows" reviews applications of swirling flows in combustion systems. Others, such as Beer and Chigier²⁴, have also performed extensive research in defining and characterizing the aerodynamics and effects of swirling flows. There are various thoughts on what is an appropriate swirl number for a premixed flame. Lefebvre²² suggests that a swirl number greater than 0.6 is appropriate for practical applications involving hydrocarbon fuels to provide adequate mixing and flame stabilization. According to Lefebvre, flows with swirl numbers less than 0.4 do not create a flow recirculation region and are referred to as weak.

In addition to the stabilization created by swirling flows, Fritz et al.¹⁵ showed that the addition of a centerbody, or fuel lance, improves the stability and decreases the chances of combustion induced vortex breakdown caused flashback. The centerbody anchors and strengthens the recirculation zone at the exit of the premixer preventing the vortex breakdown from shifting upstream due to the combustion. Also, the centerbody allows for a wider range of swirl strengths to be used because the recirculation zone no longer depends only on the vortex breakdown in the core flow.

However, there are competing factors to consider when hydrogen is the fuel. A high swirl design will incur more losses, and, as mentioned above, these losses can increase the pressure drop across the combustor and lead to extreme internal temperatures. There are various ways to impart swirl into a flow. A common method is to use swirl vanes. The vanes should be designed to minimize losses due to separation and flow turning. Careful consideration must be made when determining the swirl number that is best suited for the design. For the current design, swirl vanes were used to introduce the swirl. To minimize pressure losses, the vanes were

designed using a free vortex angular momentum distribution to satisfy a radial equilibrium condition shown in Eq. (2)²⁵, where r is the radial coordinate, C_θ is the tangential velocity, and a is constant.

$$rC_\theta = a \quad (2)$$

1.2.7 Mixing

Uniform mixing is advantageous to prevent locally rich and lean spots. Rich regions promote flashbacks and create high temperatures, which can lead to NO_x production, and lean regions promote combustion instabilities and can also lead to blowout. To prevent flashbacks, it is important that the hydrogen fuel be introduced and well mixed within a very short distance while avoiding excessive turbulence. However, this is not the case in most conventionally fueled premixers. It is common practice in natural gas premixers to introduce the fuel directly into the wakes (regions of high turbulence) of the swirl vanes, and, in some cases, the vanes themselves deliver the fuel out of the trailing edge directly into the wakes. Introducing the fuel into the wakes increases the turbulent mixing and provides an increase in lean stability. However, for hydrogen, fuel injection into highly turbulent or low velocity regions needs to be avoided. Due to extremely high turbulent flame speeds, a hydrogen flame can easily propagate or flashback into these regions in the premixer causing severe damage. Also, high momentum fuel jets introduced into the air stream can create a turbulent region that can propagate all the way to the flame zone, creating a path on which the flame can flashback into the premixer, illustrated in Figure 1.6. Plee and Mellor²⁶ explicitly discuss the effects of fuel injection into the mixing tube of a combustor creating wakes that were possibly the cause of flashbacks.

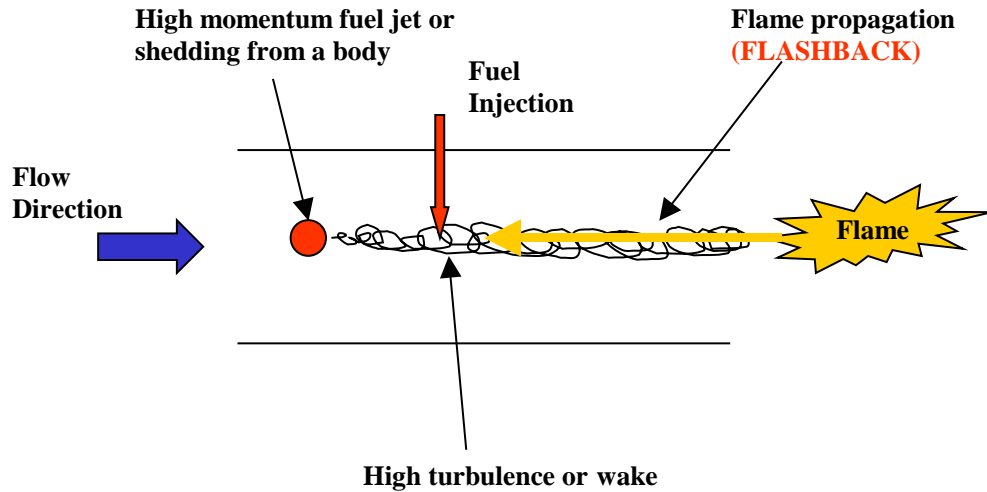


Figure 1.6. Illustration showing how introducing the hydrogen into wakes or high turbulence regions promote flashback.

Previous hydrogen premixer designs ignored one or more of the items mentioned above to try to achieve a high level of mixing in the shortest distance. Premixers designed by both Sykes²⁷ and Homitz⁷ used choked fuel injection to achieve high jet penetration and to decouple pressure oscillations created downstream from propagating into the fuel delivery system. These choked jets are high momentum jets that can create extremely rich wakes that propagate downstream promoting flashbacks. Even though some of the previous designs did achieve moderate success, they ultimately suffered flashbacks when operated at high power levels. Research, such as that performed by Holdeman²⁸, has provided useful insight into how to optimally mix jets in a cross flow. Holdeman studied many different configurations to determine optimum mixing into a crossflow. Different sizes, shapes, spacing, and orientations of mixing jets were studied at various momentum ratios (J), where subscript j represents jets and m represents mainstream flow.

$$J = \frac{\rho_j V_j^2}{\rho_m V_m^2} \quad (3)$$

Holdeman found a relationship between optimum mixing and the spacing between holes (S), the height of the duct (H_0), and the momentum ratio (J). For single side injection it was found that optimum mixing occurred when $C=2.5$.

$$C = \left(\frac{S}{H_0} \right) \sqrt{J} \quad (4)$$

1.2.8 Engine

The engine selected for modification was a Pratt and Whitney PT6A-20 turboprop engine. The engine was located at the Virginia Tech Turbomachinery Lab at the Montgomery Regional Airport. A description of the testing facilities can be found in Matt Perry's²¹ or Dan Villarreal's²⁹ Masters Thesis. This engine was selected because of the wealth of resources that were available to us on this specific engine. Parts as well as support were available from Dynamic Aviation. Also, our lab technician at the Turbomachinery Lab had been trained in operation and maintenance of this engine by Pratt and Whitney. The important aspects of the engine necessary for the design of a new lean premixed combustor that can be retrofitted into the existing engine are listed below.

A critical component of the combustor design was the compatibility with the existing turbo machinery. Physical engine dimensions, predicted flame characteristics of hydrogen combustion, and performance capabilities of existing engine components constrained the design of both the liner and premixers.

Since the goal of this project was to retrofit an existing engine with a lean premixed hydrogen combustor and because major modifications to the engine were not desirable, space restrictions were important. The only space assumed to be available in the PT6A-20 was the volume occupied by the existing Jet-A combustion liner. The liner was an annular shape with inner and outer diameters of roughly 12 and 16 inches, respectively, and a height of 8 inches. These dimensions defined the overall sizing of both the new premixers and the liner assembly.

The hydrogen premixers had multiple constraints. First, the number of premixers had to fit within the allowable space while leaving enough length for the combustion liner to dilute the hot gases to an allowable inner turbine temperature (ITT), a maximum of 800 degrees Celsius. Also, the number of premixers must be large enough to prevent large thermal variations in the gases entering the turbines. The number of premixers for a previous design used 18 injectors to achieve this; however, the most recent design only required 14. The number was coupled to the size and flame area produced by the premixer. The size of the injector was based on the desired internal velocity, the airflow through the premixer, and the allowable pressure drop. All of these things are tied together and will be explained in more detail in the premixer design section.

Chapter 2: Project Goals

The goal of this project was to demonstrate the feasibility of converting current engine technology to operate at full capacity on a clean burning renewable fuel, while producing little to no harmful emissions. Specifically, it aimed to convert an existing gas turbine engine, a Pratt and Whitney PT6A-20 turboprop, from using conventional Jet-A fuel to operating on lean premixed hydrogen. Schematics of both Jet-A and lean premixed hydrogen operation are shown in Figure 2.1 and Figure 2.2. The converted engine was to be able to produce full power (500 hp), maintain normal internal temperatures, produce zero carbon emissions, and produce near zero NO_x emissions.

To convert the existing engine, the original Jet-A combustion system must be removed. This Jet-A system uses a liquid spray at multiple points inside of a combustion liner. The liquid spray atomizes and burns in diffusion mode, while the liner introduces the air for mixing the fuel and air and for the dilution of the combustion products before entering the turbines. Burning fuels in diffusion mode, while stable and safe, produces large amounts of pollutants such as NO_x due to locally high flame temperatures. The conversion of the engine replaces this combustion system with lean hydrogen premixers and a matching combustor liner. Lean premixed combustion utilizes lower flame temperatures to minimize NO_x and uses hydrogen to eliminate carbon emissions. The modified combustion liner must appropriately split the air produced by the compressor to give the desired equivalence ratio inside of the premixers and provide adequate cooling and dilution of the combustion products. Implementation of the overall design requires proper fitting of the premixers and combustor liner within the existing engine.

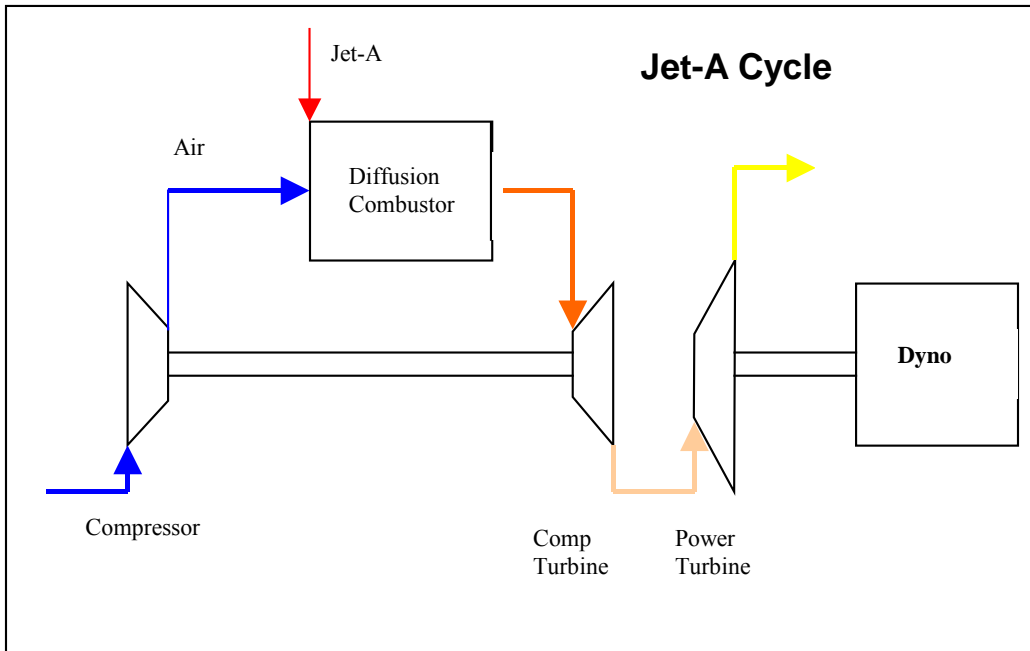


Figure 2.1. Schematic of a Jet_A fueled gas turbine engine.

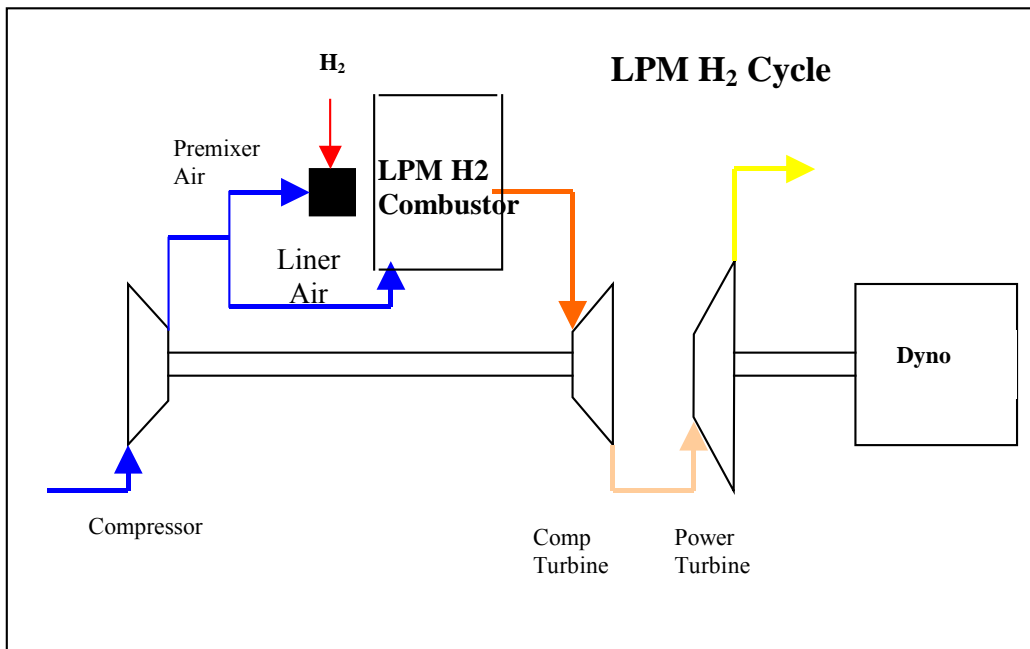


Figure 2.2. Schematic of a lean premixed hydrogen fueled gas turbine engine.

2.1 Objectives and Expectations

The conversion of the engine had three main parts, each with its own objectives and goals: 1) the design of a lean hydrogen premixer, 2) design of a matching combustor liner, and 3) the implementation of these designs into the existing engine.

2.1.1 Lean Hydrogen Premixer

- Design lean hydrogen premixer for gas turbine applications.
- Test design in controlled laboratory settings at simulated gas turbine conditions.
- Design must have a low-pressure loss to prevent increased internal temperatures.
- Design should have stable operation, no flashbacks or blowouts, under all simulated engine conditions.
- Design should achieve low NO_x levels at the designed lean equivalence ratios.

2.1.2 Combustor Liner

- Modify existing Jet-A combustion liner to operate with lean hydrogen premixers.
- Design liner to appropriately split the air so that the correct amount of air passes through the premixers to give the desired equivalence ratio to achieve low NO_x combustion.
- Build and test liner section to operate in conjunction with a premixer to ensure correct design.
- Liner should provide appropriate split, along with adequate cooling to the liner surface, and dilution of combustion products to ensure even thermal distribution before entering the turbines.
- Construct and build a new liner, by modifying the existing liner, to hold all hydrogen premixers and fit within existing gas turbine engine.

2.1.3 Engine

- Modify Pratt and Whitney PT6A-20 turboprop to operate on lean premixed hydrogen.
- Assemble engine using new hydrogen premixers along with new combustion liner.
- Construct fuel manifold and hydrogen delivery system.
- Instrument engine to monitor operation.
- Engine should have stable operation to full power (500 hp)

- Engine should experience normal internal turbine temperatures.
- Engine should produce less than 3ppm NO_x.

2.2 Thesis Outline

Chapter three describes the technical approach and methods used to design the hydrogen premixer. The premixer was evaluated and characterized by simulating its performance under engine conditions in both a computational and experimental set up.

Chapter four describes the method to create a matching combustor liner, using the findings from the premixer. It was designed to appropriately split the air produced by the engine between the premixer and liner to produce a lean equivalence ratio inside of the premixer. A liner section that matched a single premixer was constructed and tested in an experimental rig to confirm the design. The combustor liner was then constructed to the exact specifications of the design by modifying an existing Jet-A combustor liner.

Chapter five discusses some detail about the assembly of the newly constructed premixers and combustor liner into the existing engine, and the operation of the engine using hydrogen. The chapter presents the observations gathered during operation using hydrogen compared to operating on Jet-A.

Chapter six gives a summary of the entire project and provides recommendations to address the shortcomings. The summary presents the success and failures of the premixer design, the combustor liner design, and the implementation of these designs in the existing engine.

Chapter 3: Premixer

A multi-step approach was used in this project to develop a lean premixed hydrogen combustor for an existing gas turbine engine. First, the engine was instrumented and important data such as fuel flow, and compressor outlet temperature and pressure was recorded and examined. Using engine data, a model was created to provide information on parameters for on and off design engine conditions. The engine data along with the model provided restrictions and constraints on the design of the premixers, also known as injectors. A premixer concept was then modeled using FLUENT³⁰, Computational Fluid Dynamic (CFD) software, to characterize the internal flow. Then, the premixer was prototyped and fully tested to obtain its performance characteristics. The results of the tests are discussed at the end of this chapter.

3.1 Collecting Engine Data

The engine selected for modification was a Pratt and Whitney Canada PT6A-20 turboprop. It was installed and instrumented at the Virginia Tech Turbomachinery Laboratory located at the Montgomery Regional Airport in Blacksburg Virginia. Details on the testing facilities and operation of the engine on both Jet-A and lean premixed hydrogen are available Perry and Villarreal's Theses. The engine was instrumented to collect all information required for characterization such as compressor outlet temperature and pressure, combustion products, fuel flow, engine speed, and output power for the entire operating range (start-up to full power) while operating on Jet-A fuel. Using this data, a computational model was created in a cycle analysis program (Gas Turbine Simulation Program GSP³¹) so that pressure, flow, and temperature data could be calculated for on and off design operation. This model was used in the premixer design process. Because actual engine data was already recorded, this model was easily validated. For a future note, this step could be skipped if the engine manufacturer released all the information on the particular engine chosen for modification. Figure 3.1 and Figure 3.2 are plots of the important information gathered from the model. The fuel flow rate plotted is the hydrogen equivalent flow rate based on the lower heating ratio between Jet-A and hydrogen, as calculated in Eq. (5).

$$\dot{m}_{H_2} = \frac{LHV_{Jet-A}}{LHV_{H_2}} \dot{m}_{Jet-A} \quad (5)$$

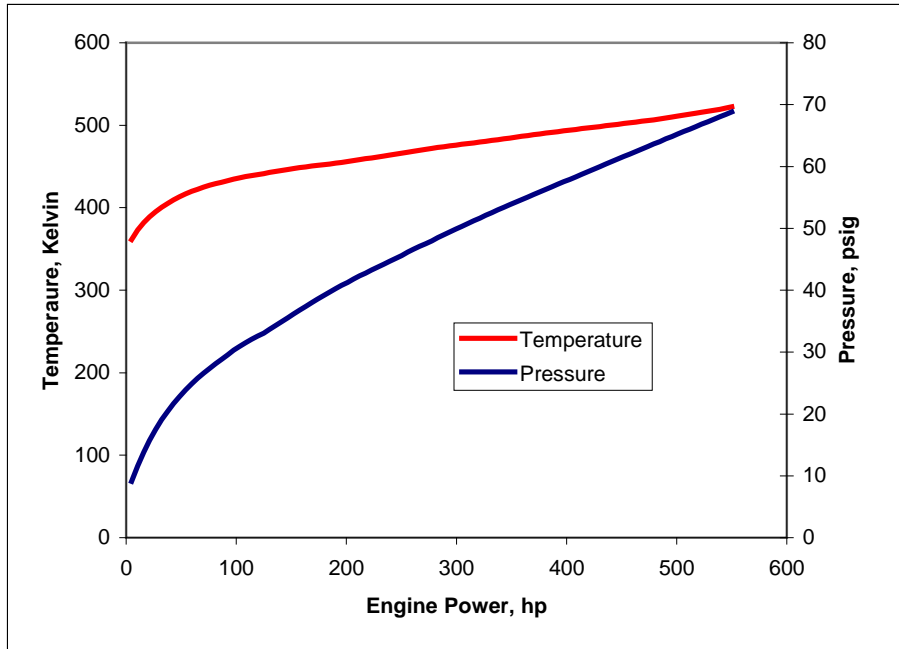


Figure 3.1. Compressor outlet temperature and pressure versus engine power level

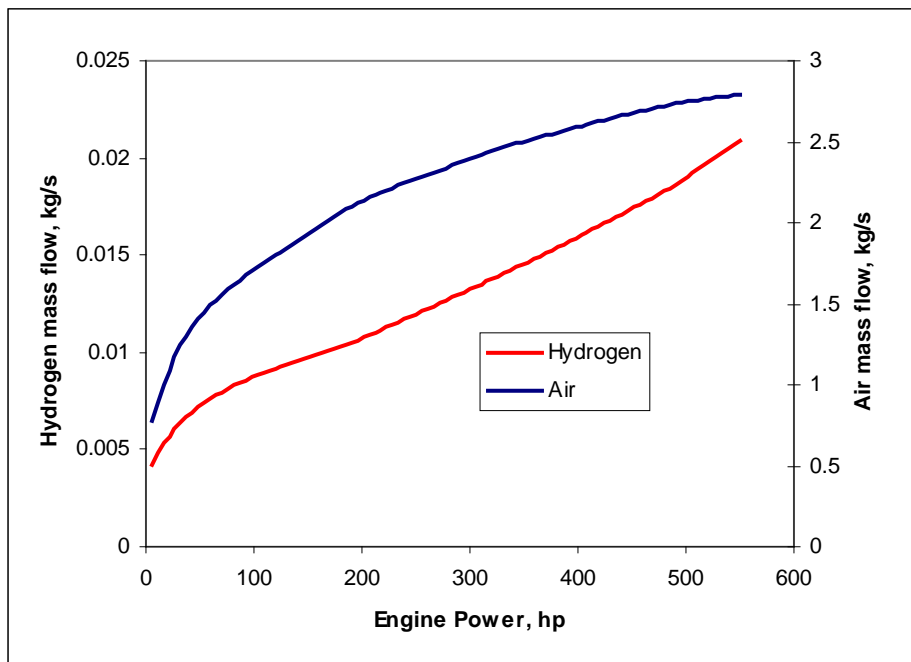


Figure 3.2. Air and energy equivalent hydrogen flow rates versus engine power.

3.2 Premixer Design

The premixer was designed to attempt to achieve all of the goals set forth in this project. Based on the PSR model presented in the introduction, the design equivalence ratio was set to be

0.4 to achieve low NO_x operation. This equivalence ratio is extremely lean for most fuels, but well within the flammability limits of hydrogen. Sykes and Homitz demonstrated that an equivalence ratio of 0.4 produced low NO_x and achieved adequate stability. To prevent high internal turbine temperatures inside of the gas turbine, the premixer was constrained to have a static pressure loss of no more than 5% through all the operating conditions of the engine. To prevent these high-pressure losses across the premixer, the internal velocity was constrained to stay between 70-100 m/s. This velocity was deemed adequate to prevent flashback from turbulent flame speed propagation in the core flow, while not incurring more than 5% pressure loss. Also, the design was limited to the use of low momentum fuel jets to prevent flashbacks due to locally rich wakes created by the fuel jets. The design also had to achieve a high level of mixing to prevent locally rich and lean regions that can promote flashback, blowoff, and combustion instabilities.

Summary of Restrictions and Constraints on Premixer Design

- Lean equivalence ratio of 0.4
- Max static pressure drop across premixer of 5%
- Internal mixture velocities of premixer between 70-100m/s
- Low momentum fuel jets
- High level of mixing

The hydrogen premixer concept created by the author has an annular mixing channel where the air and the hydrogen mix before combustion. A section view shown in Figure 3.3 and a 3-D CAD model shown in Figure 3.4 show the concept and illustrate the workings of the hydrogen premixer. The air passes through a curved (smooth) inlet to decrease entrance losses. It then enters the mixing channel created between the centerbody and outer casing. Five radial swirl vanes, extending outward from the centerbody to the outer casing, turn the flow to create swirl. The hydrogen enters from a pressurized source and passes through a tube that exits through a choked orifice into a fuel manifold. The hydrogen fills the manifold and is distributed circumferentially around the premixer. The hydrogen then passes through 10 fuel ports into the mixing channel. The hydrogen exits the fuel ports at the desired low momentum ratio into the swirling airflow where the hydrogen mixes with the air throughout the length of the mixing

channel before exiting the premixer. The mixture exits the premixer and the flame stabilizes in the recirculation zone created on the end of the centerbody.

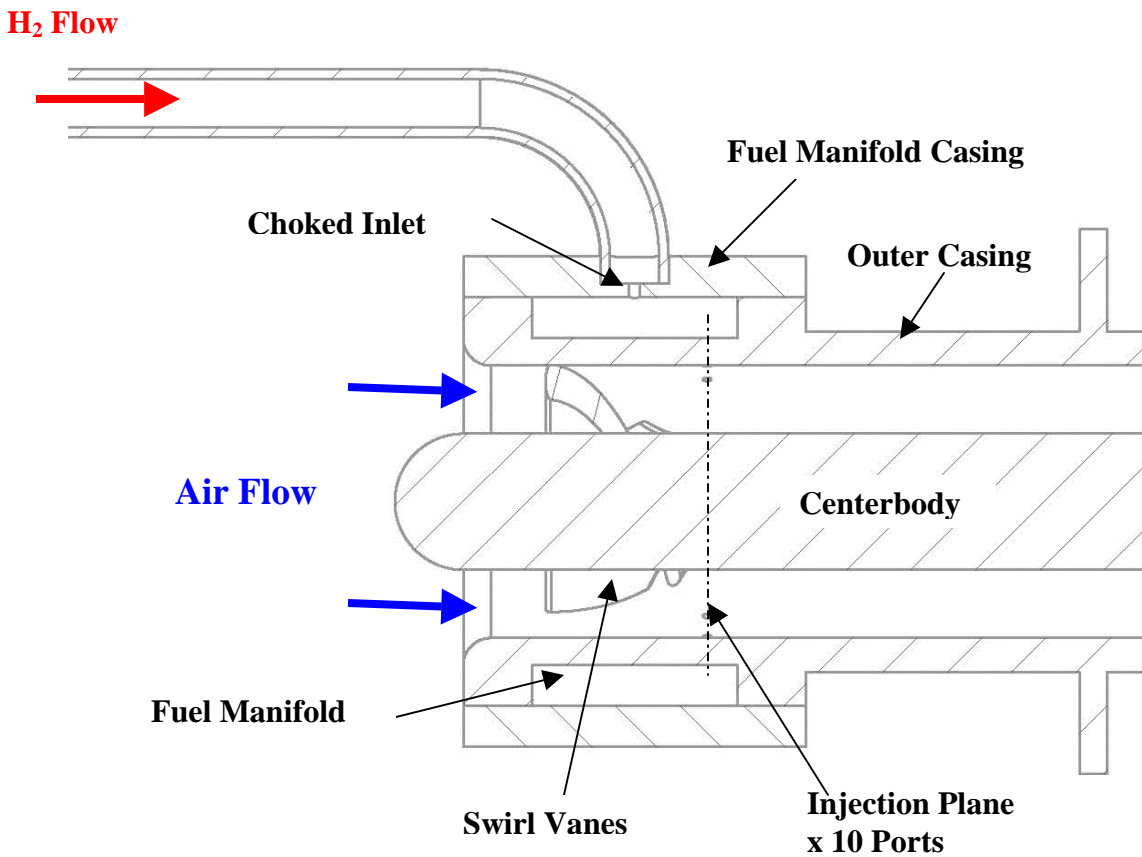


Figure 3.3. Section View of Premixer Concept

The overall size of the premixer was constrained by the physical space inside of the engine. The outer casing has a diameter of 2 inches at its largest point, and an overall length, excluding the fuel tube, of 2.75 inches. Once assembled for engine operation, the overall length, including the fuel tube and fitting, was roughly 4 inches long. This allowed approximately 4 inches for the combustor liner. The very short liner was deemed acceptable to adequately cool and dilute the hot gas stream because of the small, low temperature flame zone produced by a lean premixed hydrogen flame. Detailed drawings of the premixer can be found in the Appendix A.

The cross sectional area of the premixer was based on the equivalence ratio constraint of 0.4 (at an engine full power condition, Table 3.1) and the internal axial mixture velocity constraint of 70-100m/s. The equivalence ratio sets the air to fuel ratio. With the additional knowledge of the energy equivalent hydrogen fuel flow rate and the number of injectors considered necessary, which was 14, the air mass flow through each injector was set. The last pieces of necessary

information, from previously gathered data, were the compressor outlet temperature and pressure so air properties could be calculated. The required cross sectional area was calculated using the air mass flow, air properties, and the internal axial velocity. The internal velocity was defined as a range because the internal air velocity of the premixer will vary over the operating range due to a non-linear relationship between temperature, pressure, and airflow.

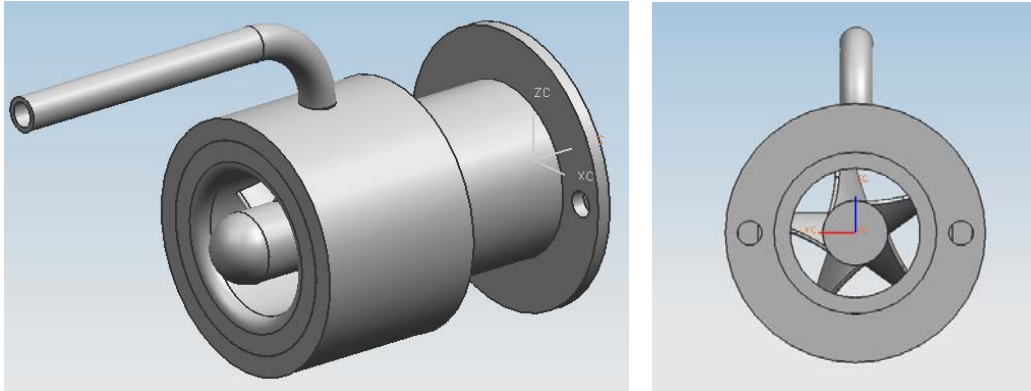


Figure 3.4. 3-D CAD models of the premixer: (left) isometric view (right) downstream exit view

Table 3.1. Engine conditions and constraints on the cross sectional area of each premixer.

500hp Engine Condition								
Power [hp]	Pressure [psia]	Temp [K]	Mass Flow H2 [kg/s]	Mass Flow Air [kg/s]	Equivalence Ratio	Area [in ²]	Number of inj	Velocity [m/s]
500	79.1	511	0.019	1.627	0.4	0.589	14	99

The diameter of the centerbody, shown in Figure 3.5, was 0.5 inches, with an inner diameter of the outer casing of 1 inch, setting the mixture channel height to be 0.25 inches. This gave an annular cross sectional area of 0.589 in². Different diameters for the centerbody and the outer casing could also be used to produce an acceptable cross sectional area. However, other considerations were taken into account in determining these diameters. The optimal mixing channel would be very thin because low velocity hydrogen jets have small penetration. To achieve this would require a larger outer casing diameter and centerbody diameter. The two problems with this are the physical space restrictions inside of the engine and the number of blades that would have to be machined to provide enough turning to the flow. Another method to achieve the same area would be to decrease the centerbody diameter. Doing this would create a very tall mixing channel that would create problems when trying to mix the low velocity

hydrogen jets. There would also be issues with machining the tall vanes onto such a small diameter centerbody.

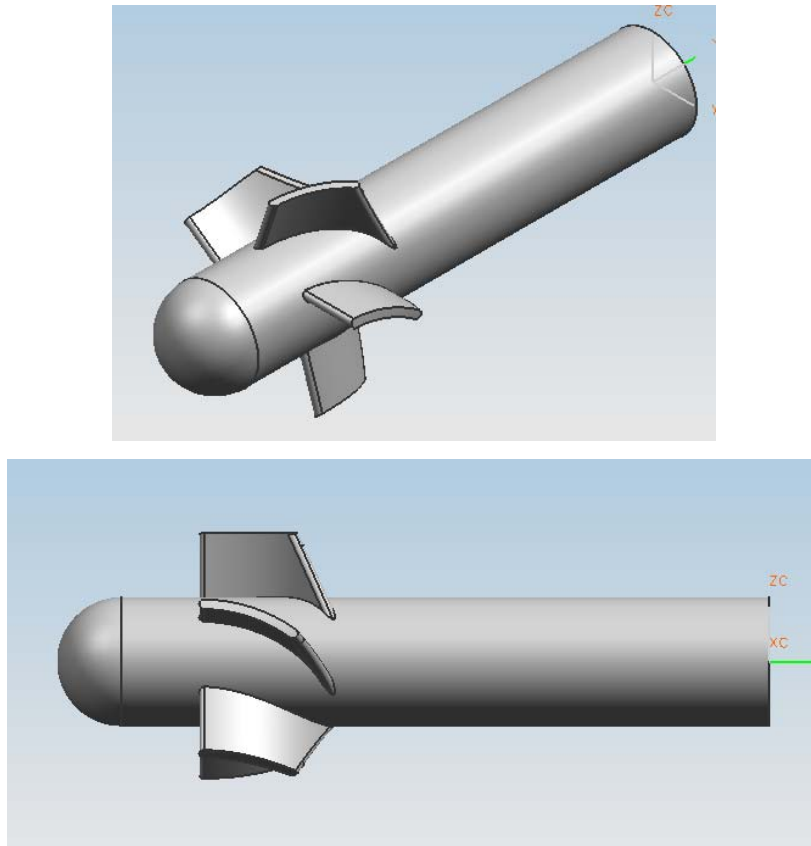


Figure 3.5. 3-D CAD models of the centerbody with vanes.

Five swirl vanes were used to create a uniform swirling flow inside of the premixer. To minimize pressure losses, the vanes were designed using a free vortex angular momentum distribution to satisfy a radial equilibrium condition, shown in Eq. (6) where r is the radial coordinate, C_θ is the tangential velocity, and a is constant.²⁵ This condition provides uniform axial velocity in the radial direction downstream of the vanes.

$$rC_\theta = a \quad (6)$$

The current vane design followed the work previously performed by Homitz and modified by Perry. Homitz used a four vane design that satisfied the free-vortex condition by using blade twist, having 60° of turning at the hub and 45° of turning at the tip of the blade, to achieve a desired swirl number of 0.6 inside the premixer. The blade height for Homitz's design was 0.12 inches, with a centerbody diameter of 0.4 inches. Perry modified the same design by using a

constant radius blade (no twist) and varying the chord length of the blade so that it would have 60° of turning at the hub and 45° of turning at the tip. Thus, the same flow turning was created as in Homitz's original design. This modification was made so that the vanes could be CNC machined instead of having to be cast. After CFD analysis, Homitz found the swirl numbers to be between 0.46 and 0.5 instead of the anticipated value of 0.6. However, the design was tested in the laboratory and demonstrated stable operation at simulated engine conditions.

Five guide vanes were needed to provide similar solidity, i.e. ratio of chord length to vane spacing, in the current premixer to the previous design. The blade height for the current design was 0.25 inches to match the height of the mixing channel. The turning angles used on the vanes to satisfy the free-vortex condition in the premixer were 60° at the hub and 39° at the tip. The current vane design incorporated Perry's modification by using a constant, 0.585 inches, radius blade with varying chord length. The blade maintained a constant thickness of 0.040 inches along the entire chord. The leading and trailing edge were rounded to provide smooth transitions to prevent separation in the flow. After CFD analysis, discussed later in the section, the swirl number was found to be 0.408 at idle and 0.413 at full power conditions.

The gaseous hydrogen fuel was introduced from a pressurized source through 1/4-inch stainless steel tubing that was welded to the manifold casing. The fuel entered the manifold through a single, 0.040-inch diameter, choked orifice. This decouples pressure oscillations created by combustion instabilities from affecting the fuel delivery rate and guarantees equal fuel delivery to all of the premixers inside of the engine. Equal fuel delivery was one of the most important aspects of the new design when compared to Homitz's original design. Homitz used eight, 0.013-inch diameter, choked orifices to deliver the fuel and provide the benefits listed above. However, due to inadequate machining tolerances, the fuel would not only be non-uniformly distributed between different premixers inside of the engine, but also the fuel delivery would not be symmetric between the eight fuel jets. This created enormous problems when trying to safely operate the engine. Premixers would have locally rich and lean zones, leading to poor stability, and the engine would have premixers that had different overall fuel flow rates that created locally hot and cool zones. This problem, in one instance, was shown to be the reason for the destruction of the compressor turbine and the inlet guide nozzles inside of the engine.

The fuel manifold was designed to act as a stagnation region for the gaseous hydrogen. The manifold was 0.75 inches long and 0.15 inches deep, with an inner diameter of 1.2 inches. This

gave an area ratio between the manifold and the injection ports of approximately 400. This assured that there should be no velocity or pressure gradients inside of the manifold, allowing for equal distribution of fuel through all ten of the fuel injection ports. Also, the inlet to the manifold was located out of plane and out of phase with the injection ports to prevent non-uniform distribution.

Another feature of the design was that the fuel was introduced from the outside of the mixing channel, unlike Homitz's design that injected the fuel out of the centerbody, or the inside, of the mixing channel. By injecting from the outside, the design takes advantage of the fact that the hydrogen has a significantly smaller molecular weight than air. When the hydrogen is introduced into the swirling air flow, the heavier molecules (air) will be forced to the outside, while the lighter molecules (hydrogen), will be drawn to the center. Homitz noticed in his studies that a large amount of hydrogen would recollect on the center body as the hydrogen approached the exit. However, instead of redesigning, Homitz simply increased the momentum ratio of the hydrogen jets to achieve a higher level of penetration into the mixing channel. The emphasis for the design in this research was to achieve a high level of mixing utilizing low-momentum fuel jets.

The location of the injection plane was designed to give the fuel maximal time to mix with the swirling air. The longer distance gave the fuel time to diffuse and mix thoroughly throughout the region, providing a uniform flame zone. The injection was placed 0.075 inches directly downstream of the vanes, which was 1.61 inches from the exit plane.

The location of the injection ports was designed so that the fuel would not be introduced into the wakes of the trailing edge of the vanes. The location of the wakes was determined using the CFD software, shown in Figure 3.6. The computational set-up can be found in Section 3.3. Two fuel injection ports were located between each pair of wakes at one-third and two-thirds the distance between the wakes.

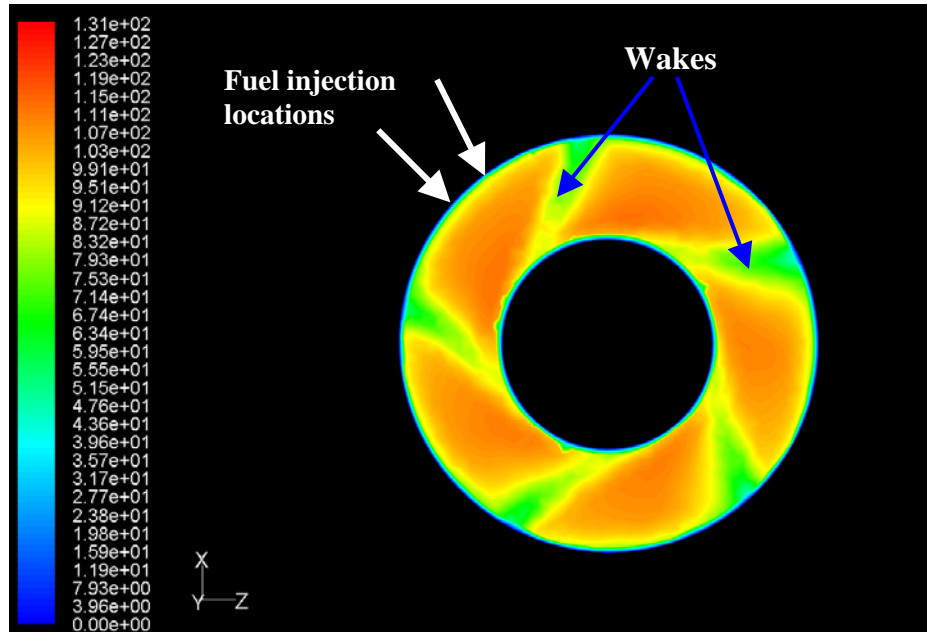


Figure 3.6. Contour plot of velocity magnitude in X-Z direction at the hydrogen injection plane at the full power condition. The wakes and location of fuel ports are illustrated.

The diameter of each fuel port was set to 0.030 inches. This diameter was determined to give the correct relation between momentum ratio, spacing between ports, and channel height to achieve optimum mixing based on Holdeman's finding for single side injection. However, slight adjustments had to be made because Holdeman's work was based on an even distribution of injection ports, and this was not the case in this design. If the ten holes were evenly spaced, the distance between each port would be 0.314 inches. However, the spacing between each port was staggered such that the two between each wake were 0.20 inches apart. At full power the total velocity, axial and tangential components, in the injection area was estimated to be about 115 m/s, as can be seen from the velocity profile in Figure 3.6. This gave a momentum ratio (J) between the fuel jets and the main air stream of 4.1. Using Holdeman's relation and assuming the holes were equally spaced gives a C of 2.54, which was as close to the optimum value of 2.5 as could be obtained by varying the diameter of the holes by 0.001-inch increments.

The fuel injection design was originally planned to be an iterative process. The design outlined above was only intended to be the initial guess. The size, number, and placement of injection ports were to be varied and optimized using CFD results obtained from multiple simulations. However, due to time constraints and the results gathered after performing simulations on the current design, it was concluded to proceed without further optimization.

3.3 Computational Set-Up

Two separate Computational Fluid Dynamic (CFD) models were created to try to completely characterize the premixer's performance. The first model examined the premixer with air being the only fluid, no hydrogen mixing. This model was used to identify the wakes coming off the swirl vanes and examine the swirl strength at the exit of the premixer. This model was simulated at both idle and full power engine conditions. The second model examined the mixing of the hydrogen inside of the premixer. This model was larger and more complex because it included mixing and a larger grid. The larger grid was necessary to analyze the recirculation zone at the end of the centerbody. The hydrogen/air model was only simulated at idle conditions because of the limited amount of convergence. Because of the shortcomings, it was decided that no conclusive evidence could be gathered by computations at higher power level conditions.

Both models used a similar process to produce a simulation of the flow using CFD software. To utilize the CFD software, the fluid volume must first be created and then segregated into very small volumes. This was done by creating a mesh over the fluid or wetted surface of the premixer. The fluid volume was created by first producing a 3-D CAD model of the premixer in *Unigraphics NX-5*.³² The CAD model was then converted into a Parasolid and imported in the meshing software, *Gambit*.³³ Since the imported CAD model of the premixer represents the solid volume of the premixer, simple shapes were created and subtracted from this volume, leaving only the fluid or wetted volume behind. Additional volumes were created at the inlet, and outlet for the hydrogen/air model, to provide a more accurate representation of the premixer in the engine environment. The volume was then split into smaller volumes so that finer meshes could be placed in areas of more complexity and interest, mainly around the swirl vanes and hydrogen inlets. Having very fine meshes over the entire volume is unnecessary and computationally expensive. Due to the complexity of the volumes, they were meshed using a Tetrahedral/hybrid mesh, type T-Grid. Shown in Figure 3.7 is a 2-D section of the grid used for the hydrogen/air CFD model. The only difference between this grid and the grid used for the air- only model was the addition of the downstream volume used to analyze the recirculation region.

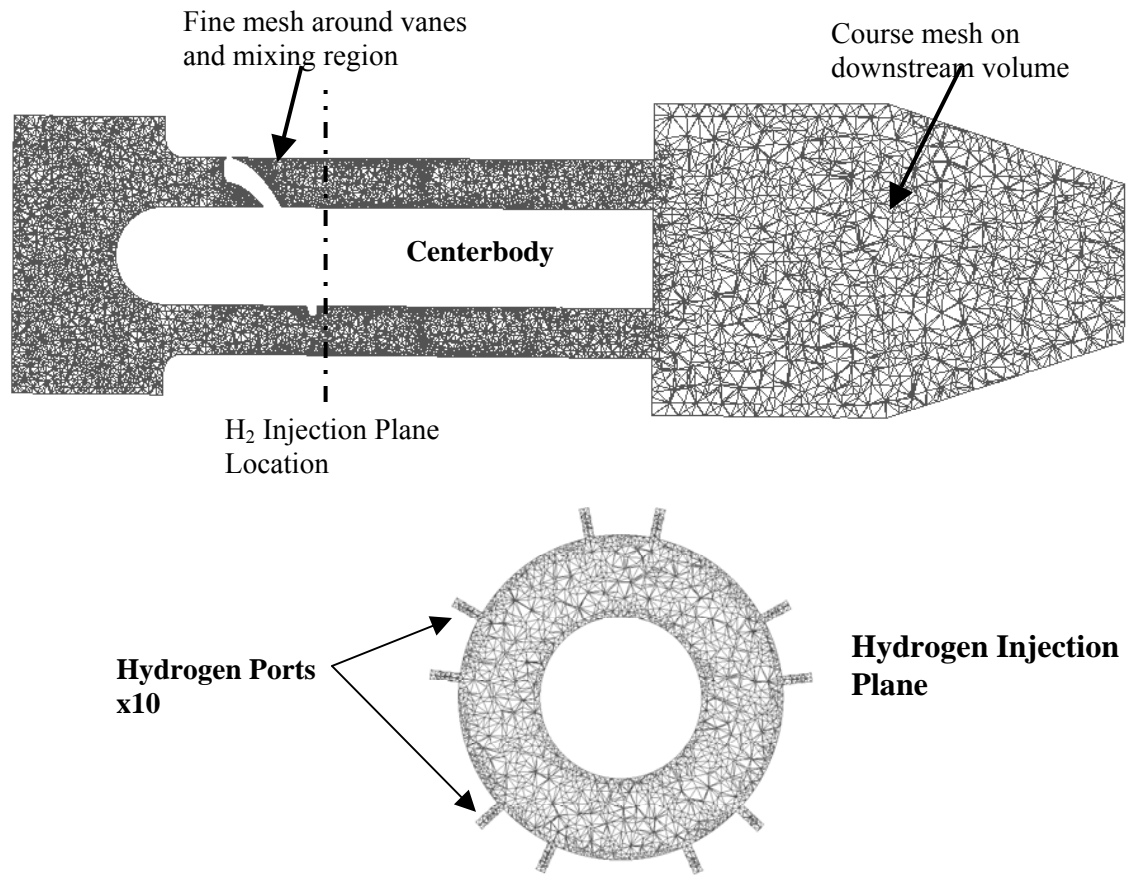


Figure 3.7. 2-D section of volume mesh, along with mesh of the hydrogen injection plane.

The meshes were then imported into FLUENT, and the solver and the boundary conditions were set for the simulations. The solver used for both cases was a pressure based steady state solver. The viscous model used was the RNG k-epsilon model using the swirl dominated flow option. This model was chosen to be the most appropriate choice for this application. From literature provided by FLUENT, this model was the best suited for simulating swirling flows with swirl numbers less than 0.5. For swirl numbers higher than 0.5, FLUENT highly recommends the Reynolds Stress Model (RSM). The solution controls were all set to second order, with the pressure-velocity coupling set to simple. During the simulation, the under-relaxation factors were continuously monitored and varied to achieve the best convergence in a minimum amount of time.

The air-only model was simulated at both idle and full power. Table 3.2 gives the boundary conditions used in the simulation. The air inlet was a mass flow inlet boundary, and the pressure outlet was set to be a pressure outlet boundary. The pressure, temperature, and flow rates were gathered from a combination of experimental data from the engine and the computer model of

the engine. The pressure set at the pressure outlet boundary was estimated to be 3% less than the inlet to the premixer, which was the compressor outlet pressure. The air was modeled as an ideal gas with constant specific heat and viscosity that was based on the air inlet temperature.³⁴

Table 3.2. Boundary conditions used in the air only simulations under idle and full power engine conditions.

Air Inlet	Idle	Full Power
Mass Flow Rate (kg/s)	0.0255	0.1162
Initial Gage Pressure (kPa)	62.95	450.9
Temperature (K)	360	511
Direction	Normal to Boundary	Normal to Boundary
Turbulent Intensity (%)	10	10
Hydraulic Diameter (mm)	38	38
Pressure Outlet		
Gage Pressure (kPa)	58	435
Backflow		
Temperature (K)	360	511
Direction	Normal to Boundary	Normal to Boundary
Turbulent Intensity (%)	10	10
Hydraulic Diameter (mm)	12.7	12.7
Air Properties		
Viscosity (N-s/m ²)	2.087E-05	2.701E-05
Specific Heat (kJ/kg/K)	1.009	1.03

The hydrogen/air model was simulated only at idle engine conditions. Table 3.3 gives the boundary conditions used for the simulation. The hydrogen/air model used the same solvers as the air model with the addition of a species transport model to account for the mixing. The species model did not involve any reactions, and it used inlet diffusion and diffusion energy source options to account for the mixing. A mass diffusivity constant was set at 4.1e-05 m²/s, and used ideal gas assumptions to account for the density, specific heat, and viscosity of the mixture. All details of the model and constants used can be found in Appendix B.

Table 3.3. Boundary conditions used for the hydrogen/air simulation under idle conditions.

Air Inlet	Idle
Mass Flow Rate (kg/s)	0.0255
Initial Gage Pressure (kPa)	62.95
Temperature (K)	360
Direction	Normal to Boundary
Turbulent Intensity (%)	10
Hydraulic Diameter (mm)	36
h ₂ Mass Fraction	0

Hydrogen Inlets

Mass Flow Rate (kg/s)	0.000299
Initial Gage Pressure (kPa)	1030
Temperature (K)	300
Direction	Normal to Boundary
Turbulent Intensity (%)	10
Hydraulic Diameter (mm)	0.762
h2 Mass Fraction	1
Pressure Outlet	
Gage Pressure (kPa)	58
Backflow	
Temperature (K)	360
Direction	Normal to Boundary
Turbulent Intensity (%)	10
Hydraulic Diameter (mm)	20
h2 Mass Fraction	0.0116

3.4 Computational Results

The air-only simulations produced valuable results with regard to the internal flow of the premixer. The most important information that was gathered from this model was the location and size of the wakes coming off the vanes, the amount of swirl imparted on the flow by the vanes. As previously shown, the wakes trailing the vanes were clearly located and were able to be avoided in the design of the fuel injection. The swirl strength was determined by calculating the swirl number at the exit of the premixer. This was done by integrating the fluxes of axial and angular momentum over the exit area. The swirl number was determined to be 0.408 at idle and 0.413 at full power. The results of these simulations are believed to be fairly accurate due to the high level of convergence, residuals approximately $10e-4$.

The main parameter that was analyzed in the hydrogen-air model was the level of mixing that was achieved by the exit of the premixer. However, a high level of convergence was never achieved. Most residuals fell below $1e-3$, but the residuals for continuity never dropped below $3e-3$ after 9000 iterations. Useful information was still gathered from this model even though it was known that the model did not reach an exact solution. From the simulation, it was apparent that injecting the fuel from the outside, even at low momentum ratios, proved to be a successful technique to transfer the fuel throughout the height of the mixing channel. Also, the location of the hydrogen jets did in fact prevent the fuel from entering the wakes coming off the guide vanes. However, from Figure 3.8, showing the contours of the equivalence ratio at the exit of the

premixer, it was clear that the fuel was not evenly distributed circumferentially around the annulus. Five distinct rich regions correspond to the five sets of two injection ports.

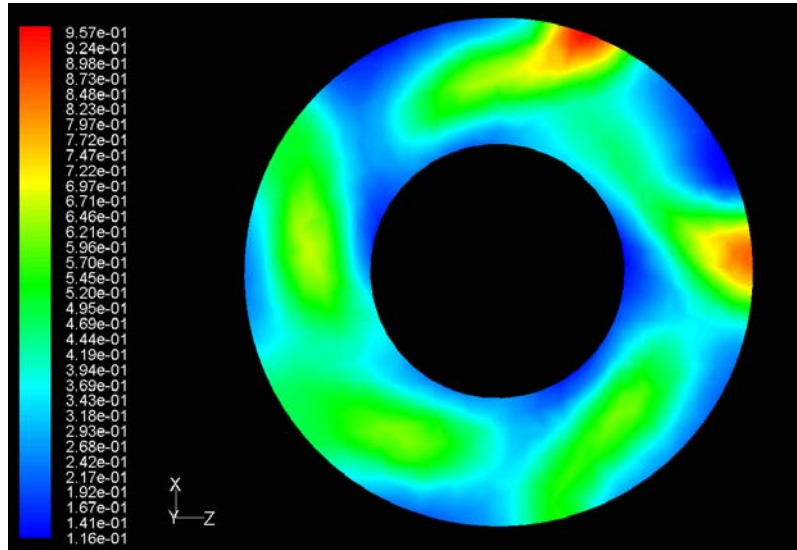


Figure 3.8. Contours of equivalence ratio at the exit of the premixer under idle engine conditions.

The hydrogen/air model was specifically created to analyze the level of mixing of the hydrogen in the premixer. The goal was to use the hydrogen mixing strategy, which has already been discussed, as a baseline for improvement. After analyzing the design, the location, size, and number of hydrogen injection ports were originally going to be varied and optimized so that the highest level of mixing could be achieved. However, due to time constraints and the lower level of convergence, optimization was not possible for this design. Therefore, no changes were made to the design before prototyping, but recommendations for optimization will be talked about in Chapter 6.

3.5 Prototype Manufacturing

The prototype consisted of four main components: the center body, the outer casing or shell, the fuel manifold casing, and the fuel inlet tube. The first three components were machined from 316 stainless steel at Custom Tool and Machining located in Salem Virginia. The fuel inlet tube was a 1/4-inch stainless steel tube.

The vanes of the centerbody were CNC machined using a ball end mill with a small step size. After machining, the vanes were then polished to provide a smooth surface to reduce losses. The main geometry of the outer casing was turned on a lathe. After turning, the ten injection holes were drilled using a 0.030-inch bit. The fuel manifold casing was first constructed using a lathe,

and then two concentric holes were drilled into the casing. The 1/4-inch outer hole provided a seat for the fuel injection tube and was not drilled all the way through the casing. The inner hole, which created the choked inlet, was drilled and then reamed to 0.040 inches to provide a very precise dimension. This precision was required for the choked inlet to provide uniform fuel distribution between premixers. The fuel manifold casing was then slipped over the outer shell and TIG (Tungsten Inert Gas) welded into place, creating the fuel manifold. The fuel inlet tube was bent using a hand held bender with a centerline radius of 9/16 inches. The tube was then inserted into the seat created in the fuel manifold casing and welded into place. It was important that all welds be checked to insure that no leaks were present. Figure 3.9 shows the machined premixer shell and centerbody as received from the machine shop

The shell and centerbody were then assembled in house. The centerbody was machined to press fit into the shell. Instead of pressing the centerbody into the shell, the shell was heated with a propane torch and the centerbody was cooled using dry ice (solid CO₂). This provided a large temperature gradient to take full advantage of the thermal expansion of the steel. The centerbody was then dropped into the casing and rotated to the correct angle, in relation to the injection holes, so that the jets were not in the wakes of the vanes. Figure 3.10 is a picture of the fully assembled premixer



Figure 3.9. Disassembled Premixer. Photo by author, 2009.



Figure 3.10. Assembled Premixer. Photo by author, 2009.

3.6 Experimental Set-Up

Once the premixer was manufactured, it was tested extensively in a modular combustor at the Virginia Tech Combustion Systems Dynamics Lab (CSDL) facility, schematic shown in Figure 3.12. The facility has the capability to test the premixer throughout the entire operating range of the engine, allowing full, independent control of air flow, fuel flow, temperature, and pressure. The combustor has the ability to run a single premixer, a single premixer in a section of the liner, or three side-by-side premixers, simulating a section of the engine's combustor as represented in Figure 3.11.

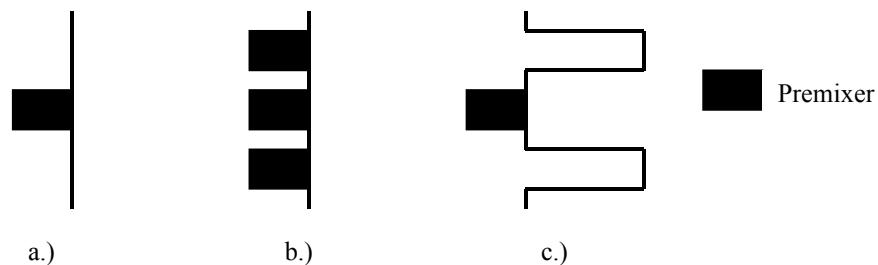


Figure 3.11. Configurations that can be tested: a.) single premixer, b.) three side by side premixers, and c.) premixer with liner section. Flow travels from left to right.

The sector combustor allowed for the investigation of a single flame, the interactions and stability between adjacent flames, or the interactions between the liner and premixer. A 150 kW

heater was used to preheat the air to simulate compressor outlet temperatures, and the rig was configured to withstand six atmospheres of pressure to simulate the internal pressure of the combustion chamber. The rig was instrumented with various thermocouples and pressure transducers to examine the performance of the pre-mixer. In addition, a Thermo Electron Model 42C High Level NO_x Analyzer sampled the combustion products to monitor the NO_x emissions.

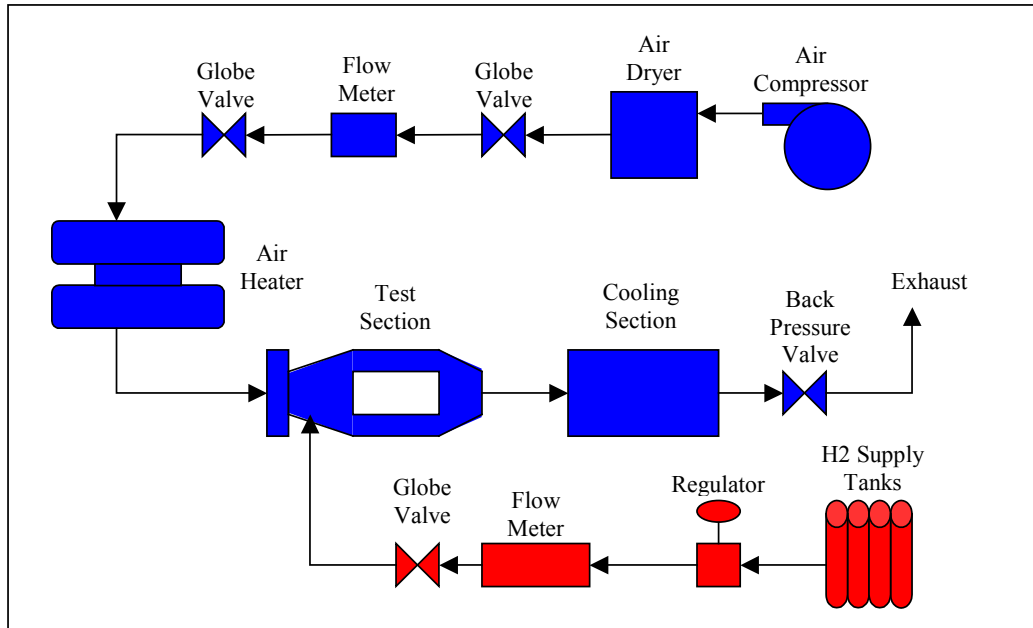


Figure 3.12. Facility at the CSDL

The facility and test set-up was very similar to the set-up used in both Homitz's and Sykes's experiments. The only major change was the redesign of the test section. The internals of the test section were redesigned to allow for the testing of the pre-mixer with a liner section. This test was not possible using the existing test section. The new design also attempted to reduce the number of air leaks in the system to allow for more accurate and more repeatable tests. The new design looked to improve upon the time needed to change the test set-up; for example, testing a different liner configuration or changing between testing a single pre-mixer and a pre-mixer with a liner.

The new test section was a variable geometry design. The design used two 3/4-inch stainless steel plates with multiple 1/8-inch wide channels milled 3/16 inches deep. The test sections could be placed between the two plates and sandwiched into the channels to form different test geometries. CAD models of the test section are shown in Figure 3.13 and Figure 3.14.

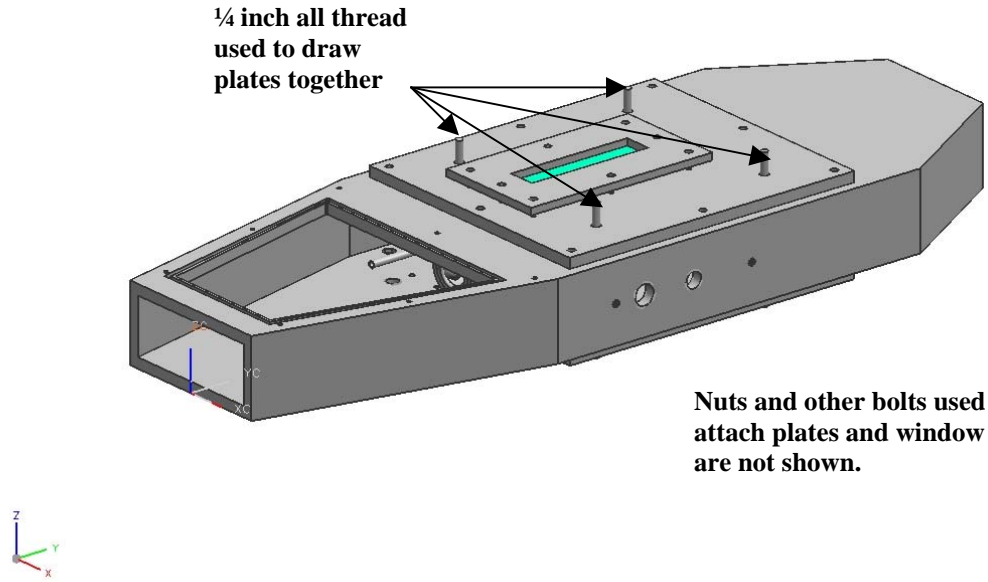


Figure 3.13. Assembled test section. Flow travels from left to right. The fuel line (not shown) would pass through a fitting and attach to the premixer.

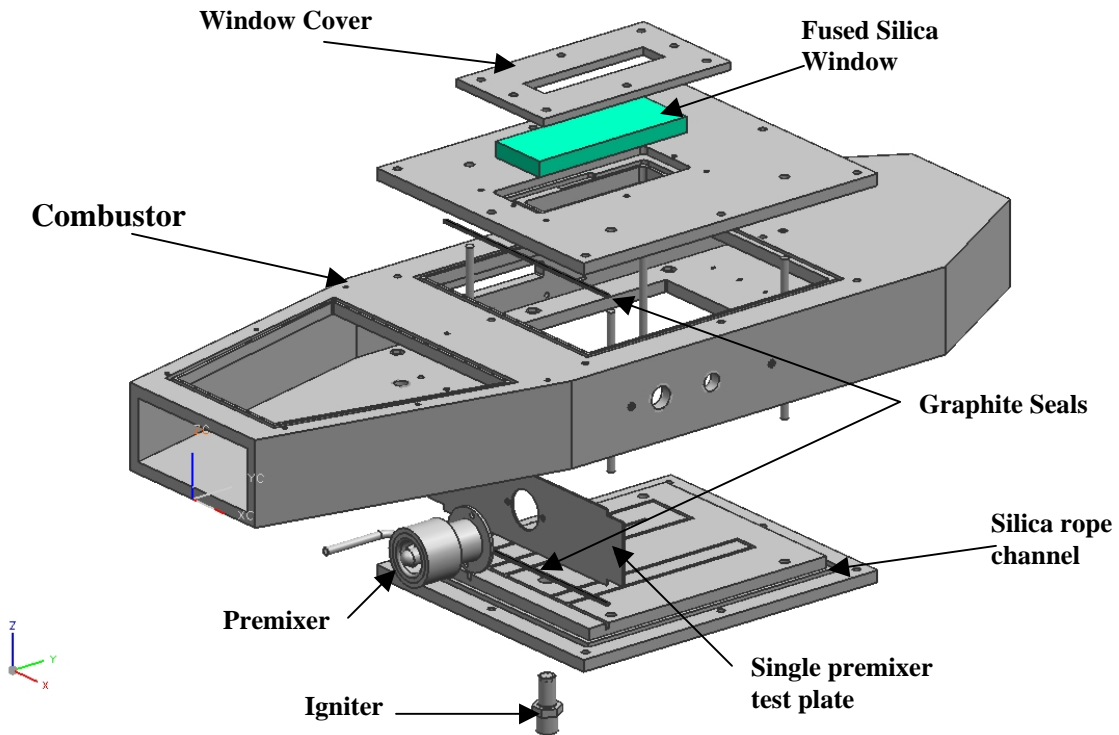


Figure 3.14. Exploded view of test section. The configuration shown is for the single premixer set-up.

The test plate was constructed out of 1/16-inch stainless steel. Holes were drilled to attach the premixer to the test plate, which also had holes to attach to tabs inside of the combustor. The igniter was passed through the back plate (plate with no window) and produced ignition directly downstream of the premixer's exit. The test plate was placed in the channels between the two plates with 1/8-inch strips of graphite laid in the bottom of the channels. At the corners of the test plate and the combustor, high temperature RTV was placed to provide additional sealing. Quarter inch braided silica rope was placed in the channels around both front and back plates to provide high temperature sealing on the outside. The two plates were bolted to the combustor with eight 10-24 stainless steel bolts each. Four pieces of 1/4-inch all-thread were passed through both plates and drawn together with nuts and lock washers. When drawn together, the graphite strips compressed and deformed to make an airtight seal and the RTV was forced into the remaining gaps on the corners. The silica rope compressed to form an adequate seal along the outside of the combustor. The fused silica window was inserted into the front plate with the same silica rope on both the plate and the window cover to providing sealing. The window was located directly downstream of the premixer to allow for visual inspection of the igniter and the flame. Detailed drawings of the front and back plates along with the window and window cover can be found in Appendix C. The assembled combustor set-up to test a single premixer at atmospheric conditions is shown in Figure 3.15, and Figure 3.16 shows the rig assembled to test at pressure.

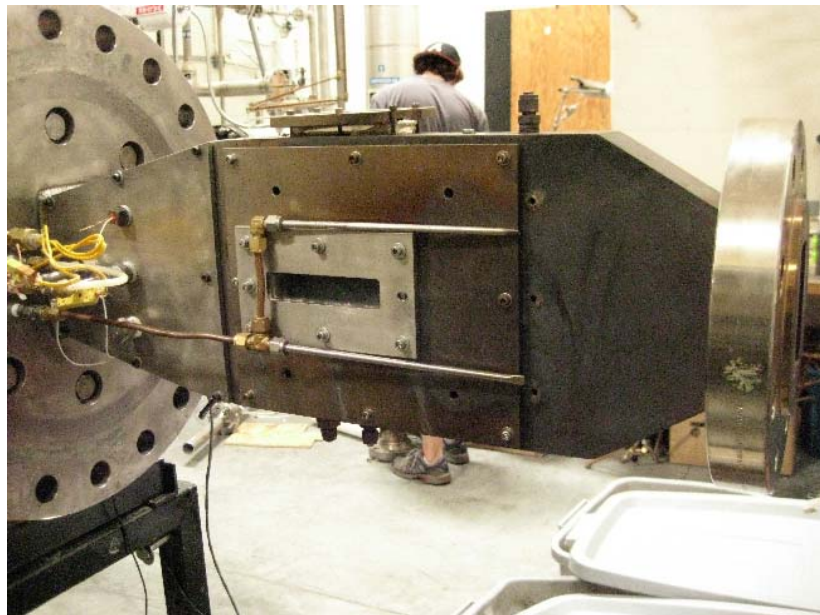


Figure 3.15. Assembled test combustor at CSDL. Photo by Dan Villarreal, 2009, used with permission.

The width of the test plate was 2.315 inches for an optimum fit in the combustor. This was determined from a previous test by measuring the amount of compression of the graphite and the silica rope. If the width was smaller, it would not seal, and if it was too wide, the plate would either bow under compression or the two plates would not be able to be drawn together enough to compress the silica rope. The optimum dimensions for the sealing channel of the silica rope were 0.25 inches wide by 0.15 inches deep. Also, because of possible deformations due to high temperatures, the front and back plates had 1/16 inches of play in all directions when fitted into the combustor.

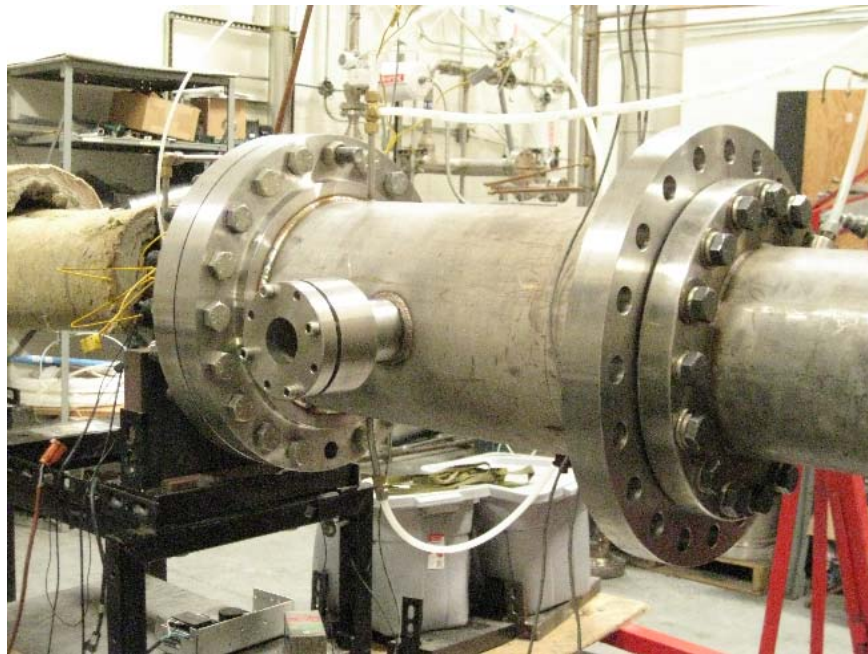


Figure 3.16. Test combustor enclosed in pressure shell to allow for high pressure testing at CSDL. Photo by author, 2009.

3.7 Experimental Tests and Results

The first test that was performed was to verify the operability of the premixer at simulated idle and low power engine conditions. The reason higher power levels were not tested at this point was due to the fact that, without the simulated liner piece being in the rig, there was an inadequate amount of cooling in the rig. Higher power tests were performed after the liner design was completed and will be discussed later. The premixer was placed inside of the rig in the single premixer setup Figure 3.11 (a). This set up allowed for the investigation of the static stability, blowoff, and flashback limits of a single premixer with no influences from other

sources. The single premixer setup was actually a worst-case scenario for stability. From a previous test with three premixers side by side, which is more representative of actual engine conditions, there was an increase in both the lean and rich stability limits. The flames help to anchor one another, providing a more stable flame zone. However, the premixers must first demonstrate an adequate amount of stability in the single premixer set up before they can be cleared for further testing.

Three engine conditions were chosen between 20 and 65 horsepower, each tested through a range of equivalence ratios. A range of 0.35-0.5 was chosen to accurately describe the range that the premixer would experience in the engine during normal operation. Because of the nature of hydrogen and past experience with premixed hydrogen systems, flashback was the main concern with the operability of the hydrogen premixer. The premixer demonstrated excellent resistance to both flashback and blowoff during all of these tests. A simple test matrix can be found in Table 3.4 with the power level corresponding to the conditions and flow rates from the engine presented in Section 3.1. Since the premixer did not experience a flashback under these conditions, it was concluded that it had sufficient stability. However, the premixer still required further investigation at higher power levels.

Table 3.4. Test matrix for static stability test at low engine power level conditions.

Power Level [hp]	Pressure [psig]	Inlet Temperature [C]	Equivalence Ratio	Flashback
21	15.8	116	0.35	N
21	15.8	116	0.5	N
38	20.5	132	0.35	N
38	20.5	132	0.5	N
65	25.7	149	0.35	N
65	25.7	149	0.5	N



Figure 3.17. Picture of flame during operation. . Photo by author, 2009.

After the static stability test was concluded to be successful, the premixer's airflow versus pressure drop was characterized. This test was performed by inserting the premixer inside the test section of pipe that was connected to a metered air source and an upstream pressure transducer, shown in Figure 3.18. The downstream side exited into the atmosphere so that the static pressure drop could be calculated from the upstream pressure, air mass flow rate, and ambient conditions. The airflow was varied through a wide range of flow rates. The flow started from zero until the flow created an upstream pressure of 30 psia upstream (sensor limit). The flow characteristics of the premixer were described using a discharge coefficient (C) calculated using Eq. (7). As can be seen from Figure 3.19, the discharge coefficient for the premixer was constant at 0.8 for all relevant Mach numbers.

$$\left(\frac{\dot{m}_{air}}{A \cdot C} \right)^2 = \frac{2P_1(P_1 - P_{atm})}{R \cdot T} \quad (7)$$

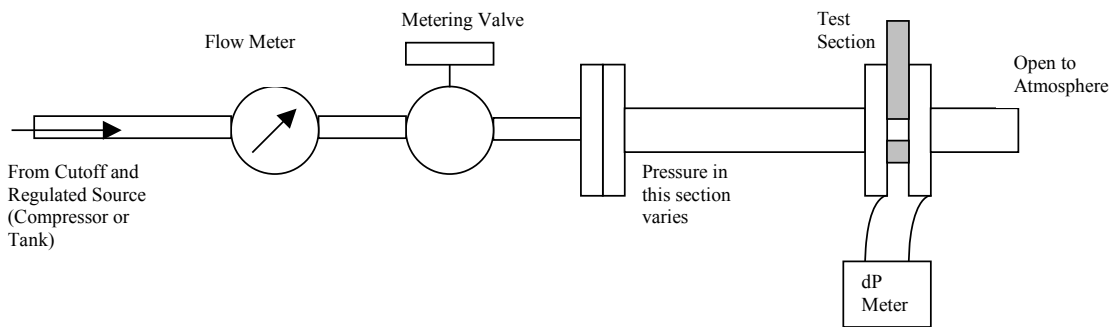


Figure 3.18. Shows the test set up to measure the discharge coefficients. Rig was used measure discharge coefficients for the premixer and for dilution and cooling holes in the liner.

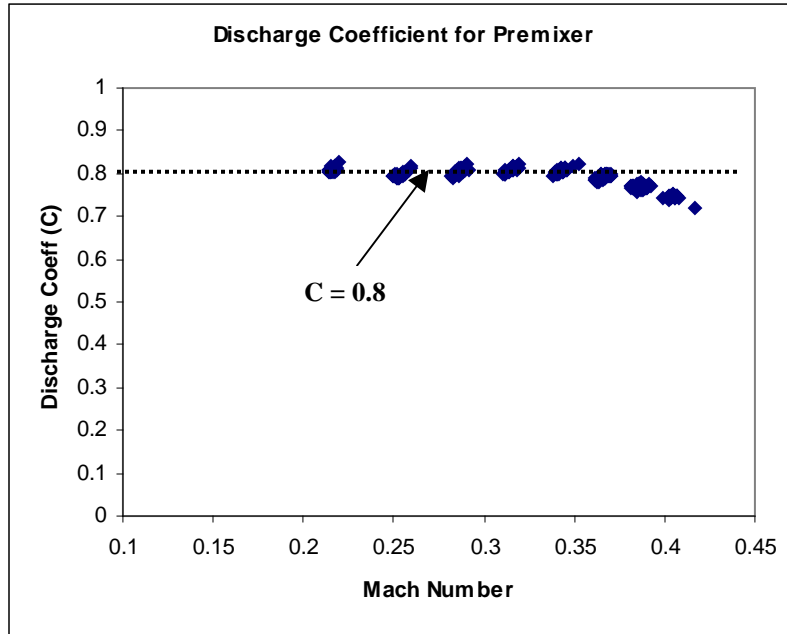


Figure 3.19. Discharge coefficient for premixer. Constant at 0.8 for all relevant flow conditions.

3.8 Discussion

Many conclusions were drawn from each aspect of the premixer’s design after examining the performance in laboratory experiments. The overall sizing, vane design, fuel injection and mixing, and flame stabilization were the main features of the design that were examined.

Many features of the premixer design were examined and quantified by visually observing the flame during operation. From the image of the flame in Figure 3.17, it can be seen that the flame is anchored very well at the exit of the premixer. This concludes that the swirl, along with the dump plane created by the centerbody, produced a recirculation zone strong enough to hold the flame. The flame appears to be of uniform length and width, meaning that the fuel is being mixed and burned evenly, radially and circumferentially. However, using a mirror placed in the flow looking straight down the flame during testing, it could be observed that the five rich zones that the CFD model predicted do exist, as can be seen in Figure 3.20. This picture qualitatively validates the CFD prediction of the mixing, shown in Figure 3.8.



Figure 3.20. Picture of flame looking down the premixer. The five rich zones that were predicted by the CFD are easily distinguishable. Photo by author, 2010.

The overall sizing of the premixer appeared to be correct by measuring the discharge coefficient and calculating the pressure drop over the entire operating range of the engine. The calculated pressure drop never exceeded 5% and the internal velocities fell between the desired range of 70-100m/s. It should be noted that the performance of the premixer in the engine would be directly related to the combustor liner design, which will be discussed later.

The performance of the vane design was measured by the pressure losses, the mixing, and the stabilization created by the recirculation zone at the exit. The pressure losses associated with the vane design are a function of both the vane shape and the amount of turning imparted on the flow. The vane shape design utilizing the free-vortex radial equilibrium condition proved to be a successful technique to minimize the losses. The amount of flow turning was characterized by the swirl number at the exit of the premixer, and was determined with the aid of the CFD model. The swirl number was found to be approximately constant at 0.41, from idle to full power conditions. According to Lefebvre, a swirl number of less than 0.4 does not produce a recirculation zone, and most practical swirlers produce a swirl number greater than 0.6. This

amount of swirl was used to produce a strong recirculation zone and enhance the mixing between the fuel and air streams. This suggests that the current design has an inadequate amount of swirl and that the turning angles on the vanes should be increased. However, there are three reasons for not increasing the turning angles in the vanes. First, a strong recirculation created by the swirl was unnecessary because the dump plane created by the centerbody helped to anchor the flame. Second, a higher swirl design would produce greater pressure losses, while maintaining the same axial velocities. These higher losses would yield the current design unusable in the engine. From CFD simulations and lab experiments, the swirling flow appeared to yield adequate mixing using the current fuel injection technique that will be discussed later. The design of the vanes is coupled to multiple aspects of the overall performance of the pre-mixer. As already stated, the pressure losses, mixing, and flame stabilization are all influenced by the vane design. The mixing and flame stabilization will be discussed in further detail later in this section. Overall, the vane design appeared to be successful in achieving adequate performance in all three areas. Further investigation into increasing the turning should be examined to determine if enhanced performance could be achieved.

The fuel injection technique was evaluated by the level of mixing achieved in the pre-mixer. A very uniform concentration of hydrogen at the exit of the pre-mixer would be considered a high level of mixing. As stated in the pre-mixer design section, the design of the fuel injection was intended to be an iterative process using the current design as the initial guess. The inability to iterate on the design proved to be a costly mistake, as it was very apparent that the fuel did not achieve a high level of mixing before exiting the pre-mixer. According to CFD results and visual observation of the flame, it appeared that the design decision of unevenly distributing the ten injection ports to avoid wakes coming off the vanes was unsuccessful. The hydrogen was never able to fully mix and diffuse circumferentially around the annulus of the pre-mixer. This led to the creation of five extremely hydrogen rich zones at the exit of the pre-mixer. The attempt to gain more resistance to flashback by avoiding the wakes was probably nullified by the increase in equivalence ratio in these rich regions. The distribution and/or size and number of injection ports needs to be changed to improve the level of mixing.

Visual examination of the flame during operation showed that using low momentum jets injected from the outside of the mixing channel successfully mixed the fuel into the air stream.

This was strictly a visual observation of the luminosity of the flame in the radial direction. However, this observation agrees with the CFD simulations presented in section 3.4.

One major issue with the premixer was the presence of combustion instability. The instability occurred throughout the entire range of operation at varying levels of amplitude. Very little research has been performed, as of yet, to characterize the instability. As mentioned before, this project did not study the dynamic stability of the flame but acknowledged the influence instability of this nature could have on the creation of flashbacks in a premixed system. More information on the research that was performed, and the results obtained from that research can be found in Chapter 6.

Air flow leaks proved to be an issue in previous experiments. The design of the new test section for the experimental rig exhibited improved performance when compared to the existing rig used in Sykes and Homitz experiments. Pressure versus flow tests revealed that the rig greatly reduced the amount of air leaks during the experiment. A solid test piece was inserted into the test section in the place of the premixer. Then the airflow was increased until there was a 2 psi pressure drop between upstream and downstream of the test piece. The difference in airflow was then compared to the airflow required to create the same pressure drop when the premixer was in place. The amount of air that leaked past the experiment was measured to be about 5%. This was a huge improvement over the existing design, which had almost 50% leaks. Reducing the leaks improved the accuracy of the equivalence ratio measurement inside of the premixer by the same percentage, because the airflow is directly related to the equivalence ratio. The operation of the rig also demonstrated to be very repeatable when disassembled and reassembled. This was determined by frequently performing this pressure versus flow test.

The premixers were machined with precision and care. The premixers were all flow tested to be within 10% of one another to ensure equal distribution of fuel. All premixers were pressure tested to check for leaks in any of the welds. A few small leaks were found, but they were easily fixed. Symmetric distribution of fuel around the ten fuel ports was visually checked by submersing the premixer in water and flowing air through the fuel line. This test confirmed that all the small fuel ports were very precisely machined. Excellent work was done on machining and polishing the vanes. In all cases, the press fit between the vanes and the premixer shell was perfect. Overall, the author was very pleased with the attention to detail and level of care taken in creating these components.

Chapter 4: Combustor Liner

After the premixer was designed, the liner was designed to correctly match the premixers with the engine. The total air produced by the compressor must be split correctly between the liner and the premixers. The air that passes through the liner must provide adequate cooling of the liner walls and dilute the hot gas stream to an allowable turbine temperature. The air that passes through the premixers must be the appropriate amount to create the desired equivalence ratio. Inside of the engine, the compressor delivers a set amount of air that depends on the compressor speed and the pressure drop of the combustor. The compressor speed is directly related to the amount of fuel energy entering the system. From both measured and modeled engine data, the total airflow rate for the given fuel flow rate was known along the entire operating range of the engine. Knowing the premixer performance, total air flow, and the fuel flow, the liner was designed to passively control the air flow split between the liner and the premixers to produce an equivalence ratio of 0.4 at the full power engine condition.

4.1 Combustor Liner Design

Instead of constructing a completely new liner, this project simply modified an existing combustor liner, Figure 4.1. The requirements for the new liner fit nicely with modifying the original Jet-A combustion liner. Relatively minor modifications were sufficient to create exactly what was needed. Due to the space restriction, as discussed in the Introduction, the liner had to be cut down to allow enough space to insert the new premixers. Out of the original 8-inch long liner, only the last 3.4 inches were kept. The inner and outer diameters were not changed so that the liner would fit inside the engine in the same manner as the original. It was possible to cut the liner down because of the much shorter flame length of the premixed hydrogen when compared to the Jet-A diffusion flame.



Figure 4.1. Original combustor liner for the PT6 turboprop engine using Jet-A fuel. Photos by Dan Villarreal, 2009, used with permission.

The design of the new liner began with fully characterizing the flow properties of the 3.4-inch section of the existing liner, since that was the reused piece within the new design. In this remaining 3.4-inch section, there were seven rows of dilution and cooling holes. The row of primary dilution holes for the Jet-A configuration consisted of 30 0.375-inch diameter holes. This row of holes had to be blocked by welding inconel plugs into each hole and, therefore, was not characterized. The remaining six rows of holes were splash-ring style cooling holes to cool the liner, and all were kept and characterized for the new design. Splash-rings use only the static pressure of the upstream air to force cooling air through the outside of the liner onto an internal deflector, shown in Figure 4.2. The deflector, also called a baffle or lip, creates a sheet of cooling air directed along the wall of the liner. This sheet of air protects the liner from the hot combustion gases. More information can be found on the heat transfer and aerodynamics of these and different cooling designs in “Gas Turbine Combustion” by Lefebvre.²² These rows of film cooling holes were characterized in the same way as the premixers, by using a constant discharge coefficient. Sections of a spare Jet-A combustor liner were cut out and adhered to plates that could be inserted into the same rig, shown in Figure 3.18, and they were tested in the exact same manner as for the premixer.

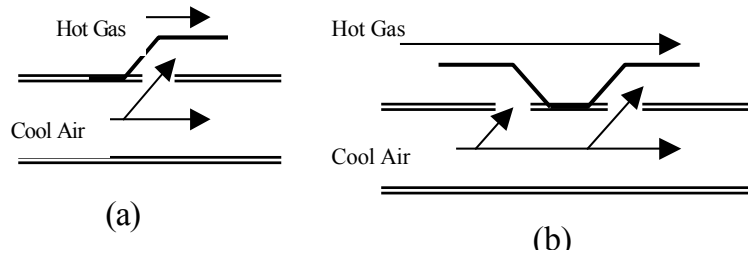


Figure 4.2. (a) Splash ring style, (b) double splash ring style cooling holes.

There were four test sections because two sets of holes were double splash rings. Table 4.1 shows the results from these experiments along with the premixer result. The description refers to the piece that was tested inside of the rig. The ID and OD indicate whether the holes were located on the inner or outer portion of the liner, and double refers to if the piece tested contained two rows of holes. For example, the set of five 0.125-inch holes (ID) means that a section of liner, taken from the inside, contained five holes that were each 0.125 inches in diameter. Also, since this was only a small section of the liner, there were 24 sets of these in the actual liner, meaning there were 120 total holes of this size in the liner. The area refers to the total area of the tested piece, in this case five 0.125-inch diameter holes. The discharge coefficient, C , was calculated using the same equation as for the premixer, Eq. (7). From previous experience with the liner design, it was known that additional holes were needed so that the liner would correctly match the premixers. However, neither the size nor the number of holes that were required was known at this point. Therefore, the last pieces of information that needed to be collected were the flow properties of standard sized holes that could be added to the liner to achieve the correct properties. Three standard hole sizes, 1/16, 1/8, and 1/4 inches, were tested and characterized in the same fashion as the liner sections and the premixer. Three different plates, each with a particular size of holes, were placed inside the test rig, as seen in Figure 3.18, and tested.

Table 4.1. Discharge coefficients for the premixer, 6 rows of splash ring cooling holes, and 3 standard sizes.

Description	Number/Sets	Area (in ²)	C
Premixer	14	0.589	0.8
Set of 5 1/8inch holes (ID)	24	0.061	0.6
Set of 3 1/8inch holes (OD)	37.333	0.037	0.63
Set of 6 0.078inch holes (double ID)	40	0.029	0.62
Set of 6 (3 0.0635 and 3 0.082) inch holes (double OD)	60	0.025	0.69
1/16 inch hole	1	0.0031	0.67
1/8 inch hole	1	0.0123	0.71
1/4 inch hole	1	0.1963	0.58

The process to design the liner so that the flow was appropriately divided between the premixers and cooling holes was relatively straightforward. The only unknown in the design was the number and size of holes to add to the liner so that the equivalence ratio was 0.4 at 500 hp. The parameters at 500 hp are shown in Table 3.1. The first step was to calculate the air mass flow rate required to achieve an equivalence ratio of 0.4 inside the premixers using Eq. (8).

$$\dot{m}_{air} = \frac{\dot{m}_{H_2} \frac{1}{2} (4.76) MW_{air}}{\phi \cdot MW_{H_2}} \quad (8)$$

The resulting airflow rate through the premixers, \dot{m}_{air} , was 1.627 kg/s, which is 59% of the total air. Using the discharge coefficient that was already established, the static pressure drop across the premixers was determined to be 2.849 psi using Eq. (7). This corresponds to an overall pressure drop of 3.6%, which was within the prescribed constraint of 5%. This sets the split to be 59% premixer to 41% liner air, shown in Figure 4.3.

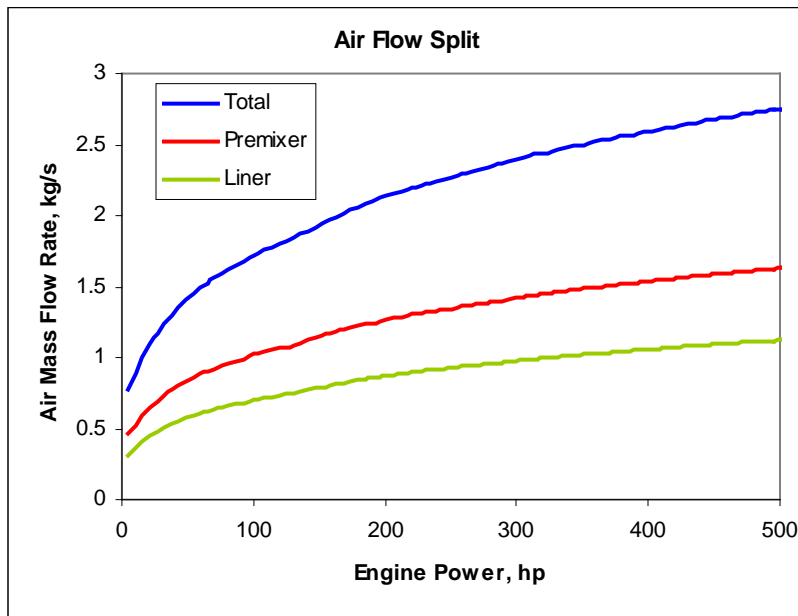


Figure 4.3. Air flow split showing total air produced by compressor, air flow required for premixer operation (59%), and air flow through combustor liner (41%). Percentage is in reference to total air flow.

Because the liner and premixers have the same upstream conditions and exit into the same volume, the pressure drop across the liner has to be the exact same as the pressure drop across the premixers. Therefore, the liner had to be designed to allow the remaining air ($2.747 - 1.627 =$

1.12 kg/s) to pass through the liner with a 2.849-psi pressure drop. Rearranging Eq. (7), and using all the previously gathered discharge coefficient information, it could be determined that 119 1/8-inch dilution holes had to be added to the liner to correctly match the liner to the premixers, as shown in Eq. (9). The summation term was the addition of all of the existing rows of holes, and the subscript of 1/8 refers to the 1/8-inch holes.

$$\dot{m}_{liner} = \sqrt{\frac{2 \cdot P \cdot \Delta P}{R_{air} \cdot T} \left(\sum_i (n_i A_i C_i) + n_{1/8} A_{1/8} C_{1/8} \right)} \quad (9)$$

The liner was designed at a single operating condition. However, the design must be simulated at all operating conditions (idle to full power) to ensure successful operation of the engine. As noted before, it was known that the equivalence ratio along the operating range would vary due to changes in compressor and turbine efficiencies along with a bleed schedule. Large variations that could create far off design conditions were of concern and in need of investigation. Certain conditions such as high/low internal velocities or equivalence ratio could cause blowout or flashback. Also, at no point in the simulated operating line could the pressure drop climb above 5 %.

The following data in Figure 4.4 and Figure 4.5 show that the design was suitable for engine operation. The internal velocities of the air and the fuel air mixture, Figure 4.4, fell within the constraint of 70-100m/s. In addition, at no point along the operating line did the pressure drop exceed 5 %. The data in Figure 4.5 show a large variation in equivalence ratio along the range of engine conditions. This is due to the non-linear relationship between the fuel input and the airflow generated by the compressor. This equivalence ratio variation presented an operational challenge. The equivalence ratio at low power levels dropped below 0.3, which was too low to sustain a flame for a single premixer. This was unavoidable for lean premixed operation throughout the entire operating range while maintaining the constraint of 0.4 at full power. However, this design was deemed acceptable for the reasons that are explained later in the Discussion section of this chapter.

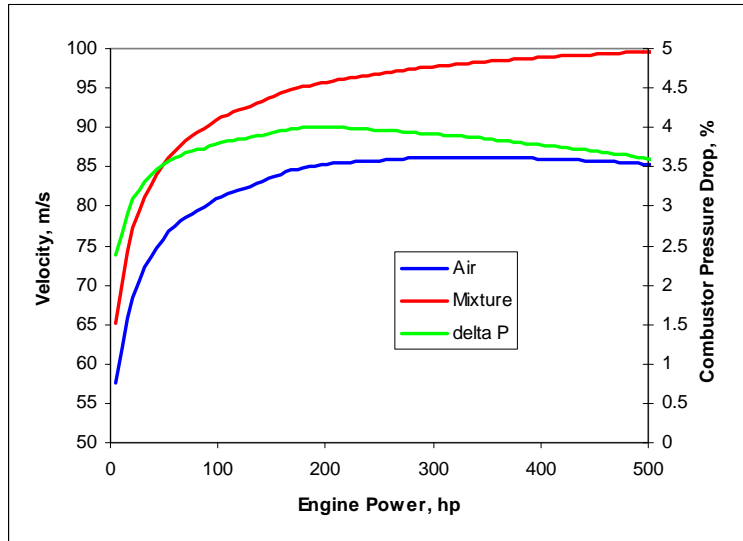


Figure 4.4. Predicted premixer internal air and mixture velocities with corresponding pressure drop across the premixer, all versus power level.

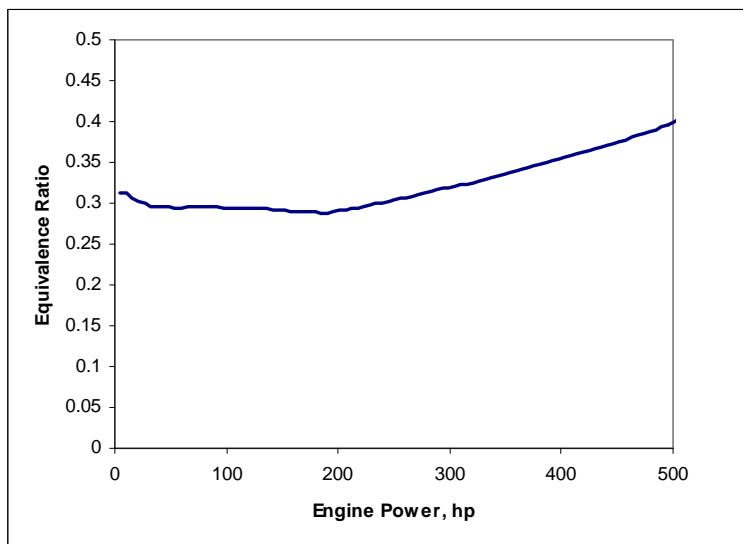


Figure 4.5. Predicted equivalence ratio

4.2 Testing of Combustor Liner Section with Premixer

Once the preliminary design was completed and deemed acceptable, a liner section prototype was constructed for testing. The liner section prototype was a 1/14 rectangular section that could be fitted into the combustion test facility and tested with one premixer. The test section was assembled in the same fashion as discussed earlier for testing the single premixer. This section simulated the section of the liner that corresponded to one premixer. The liner section was constructed out of stainless steel instead of inconel due to the cost of the material. Also, since stainless steel has a lower melting point than inconel it would be easier to conclude if there was

adequate cooling provided by the splash rings and the additional 1/8-inch holes. The liner section was completely built in house so that changes could be made relatively quickly. The liner wall was drilled to the exact dimensions of the existing liner, and splash rigs were TIG welded into place. The additional dilution holes were not added to the walls of the liner, but instead were only added to the back plate that was custom built to hold the premixers. This configuration kept the airflow that was exiting the dilution holes from directly impinging on the flame, which had not been characterized and could possibly affect the stability of the flame. The test set-up is shown in Figure 4.6.

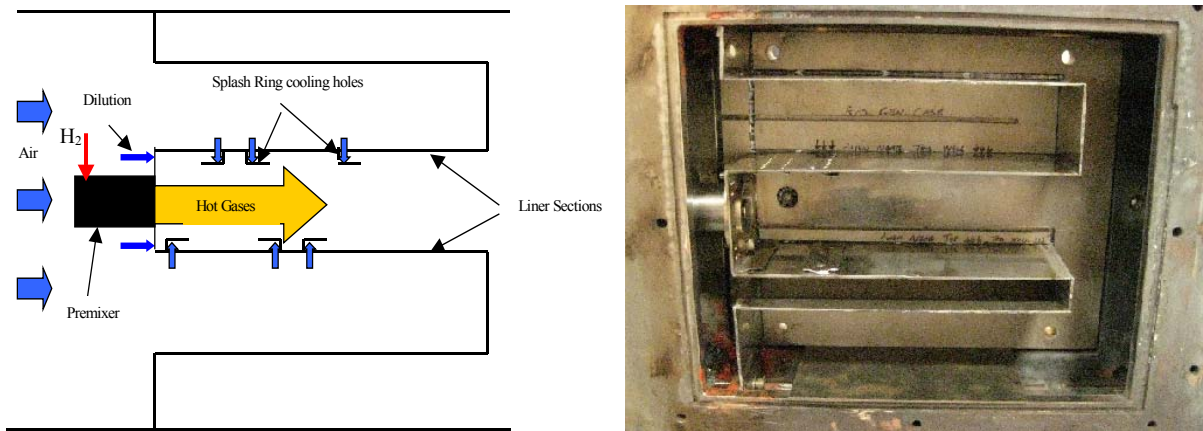


Figure 4.6. Schematic and picture of test set-up. Photo by author, 2009.

The premixer and liner assembly were tested through the operating line of the engine. The operating line matched the compressor outlet pressures, temperatures, and total air flows as predicted by the model. Only the upstream conditions were controlled in these tests, forcing the liner to appropriately split the air between the premixer and itself. Table 4.2 gives the operating conditions used in these tests. At low power conditions, the flame was unable to become stable due to blowoff, and had to be slightly richened to sustain a flame. For example, point (1) in Figure 4.7 is slightly above the operating line representing these conditions. As stated before, this was expected and accounted for. For the majority of the operating line, the premixer demonstrated excellent stability. The 500 hp (max) engine condition was the only condition in which the premixer experienced a flashback. The pictures in Figure 4.7 show the flame at a few selected points along the operating line.

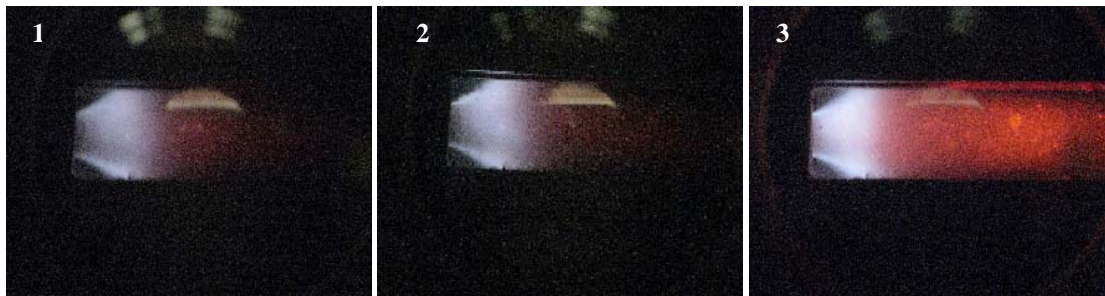
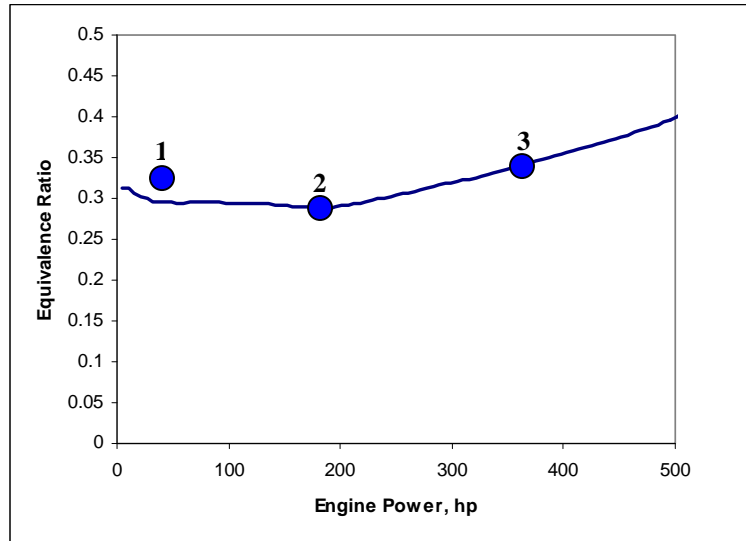


Figure 4.7. Flame picture along the actual operating line. (1) 38hp 0.33 eq ratio (2) 190hp 0.29 eq ratio (3) 365hp 0.34 eq ratio. These 3 conditions give a good representation of flame structure at low, medium, and high power conditions, respectively. Photos by author, 2009.

Table 4.2. Test conditions and stability results for the liner section with the premixer.

Power Level [hp]	Press [psig]	Temp [C]	Air Flow [scfm]	Fuel Flow [scfm]	Equivalence Ratio	Stability
idle	9.1	88	95	7.7	0.31	Blowoff
21	15.8	116	135	10.5	0.3	Blowoff
38	20.5	132	161	12.2	0.3	Stable
65	25.7	149	188	14.3	0.3	Stable
98	30.3	162	210	16	0.3	Stable
147	35.6	173	237	17.8	0.29	Stable
190	40.3	181	260	19.3	0.29	Stable
245	45.1	192	279	21.7	0.3	Stable
305	50.3	204	297	24.5	0.32	Stable
365	55.1	214	312	27.5	0.34	Stable
430	60	225	326	30.8	0.37	Stable
500	65.2	238	339	34.9	0.4	Flashback

By examining the shape, strength, and stability of the flame, it was concluded that the liner was providing the appropriate split of the total air. After fully testing the liner with the premixer, the test section was disassembled and examined for damage. No thermal damage was observed on either the liner section or the premixer. These results concluded that the combustor liner was properly designed to split the air, and the splash rings provided adequate cooling for the combustor walls.

4.3 Combustor Liner Manufacturing

As mentioned before, the liner was constructed by modifying a PT6A-20 original equipment combustor liner. The combustor liner was laser cut 3.4 inches above the base of the liner on both the inner and outer surface of the annulus. The inner and outer radii were exactly measured after cutting, and the liner plate was cut out of a 1/16-inch inconel sheet to fit between the pieces. The liner plate, show in Figure 4.8, consisted of 14x1.26-inch laser cut holes for the premixers, 4x0.5-inch laser cut holes for the igniters, and 168x0.125-inch laser cut dilution holes. The premixer holes were cut 0.01 inches larger than the premixer to allow room for thermal expansion. The igniter holes were cut off center to allow room for the premixers, and the linear spacing of the dilution holes was kept constant on the inner and outer radii of the plate to provide uniform dilution and cooling (98 outside and 70 inside). Notice that the design only called for 119 dilution holes, but more holes were needed because the flange on the premixer blocked approximately 3.5 holes per premixer. Two of the dilution holes per premixer were used to attach the premixer to the combustor liner with number 6 bolts and locking nuts.

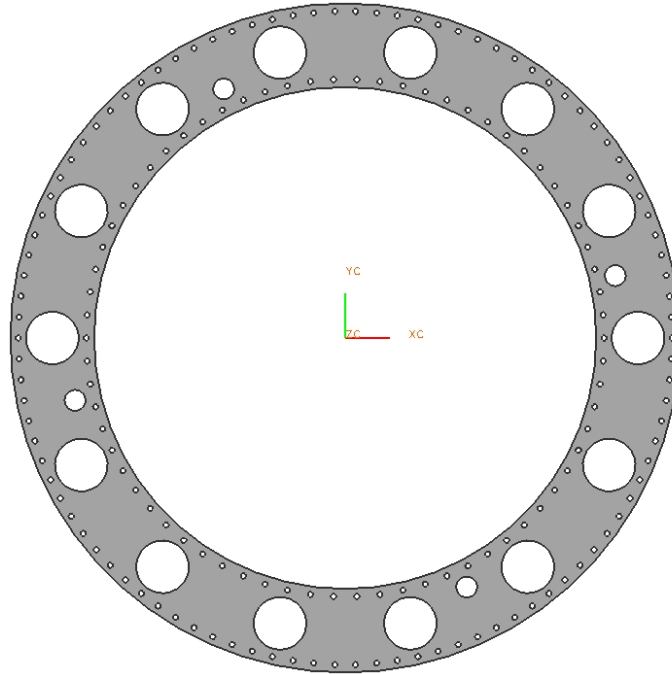


Figure 4.8. Inconel liner plate designed to hold 14 premixers, 4 igniters, and 119 unblocked dilution holes.

The liner plate was TIG welded between the two 3.4-inch tall liner sections leaving an annular shaped combustor liner that could fit exactly into the existing engine. Thirty 3/8-inch diameter plugs were cut out of 0.040-inch inconel and welded into the liner to block the dilution holes, shown in Figure 4.9. The finished combustor liner can be seen in Figure 4.10.

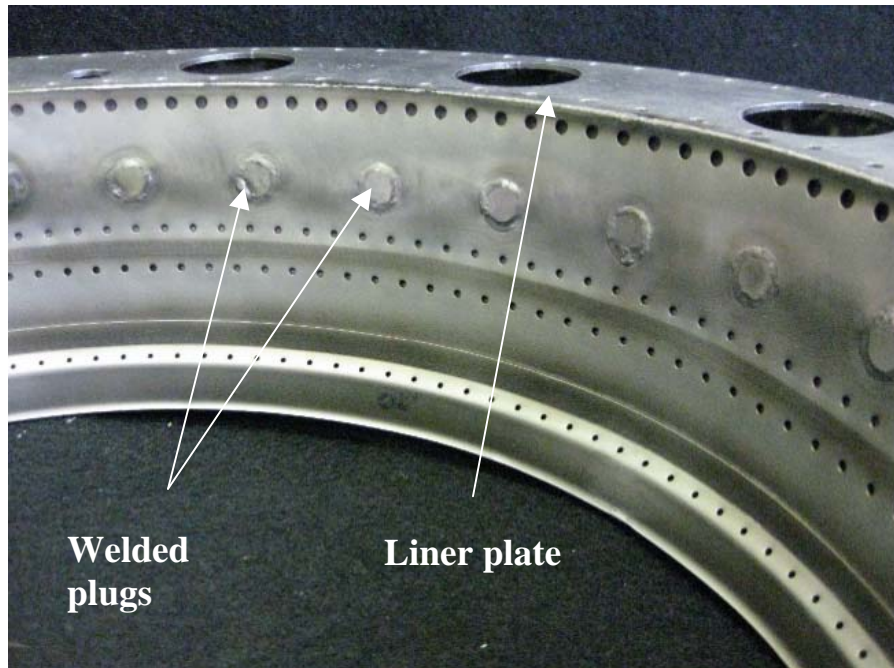


Figure 4.9. Picture showing the welded plugs and weld holding the liner plate. Photo by author, 2009.



Figure 4.10. Lean premixed hydrogen combustor liner. Photos by author, 2009.

4.4 Discussion

The combustor liner design was deemed acceptable despite the low equivalence ratios at startup and low engine power for two reasons. First, even though an equivalence ratio of 0.3 could not sustain a flame for a single premixer, it might be able to operate in a ring of premixers because of the added stability created by adjacent flames. Second, because this design does incur slightly more pressure drop than the original 2%, it can be theorized that there may be a slight decrease in overall airflow rate. This decrease in airflow would cause an overall richer mixture, which could create stable operating conditions. Keeping these two conditions in mind, in general, it was safer to design on the lean side of stability because it provides more room for adaptation. For example, if the design cannot sustain a flame at low power levels, additional holes could be added to the liner to richen up the mixture. Pilots are also an option to help accelerate the engine to a condition where the premixers could self sustain. Also, the premixers could be turned on in stages, shown in Figure 4.11. By not turning on all of the premixers at once, it divides the same amount of fuel through a smaller number of premixers, causing the fueled premixers to be richer.

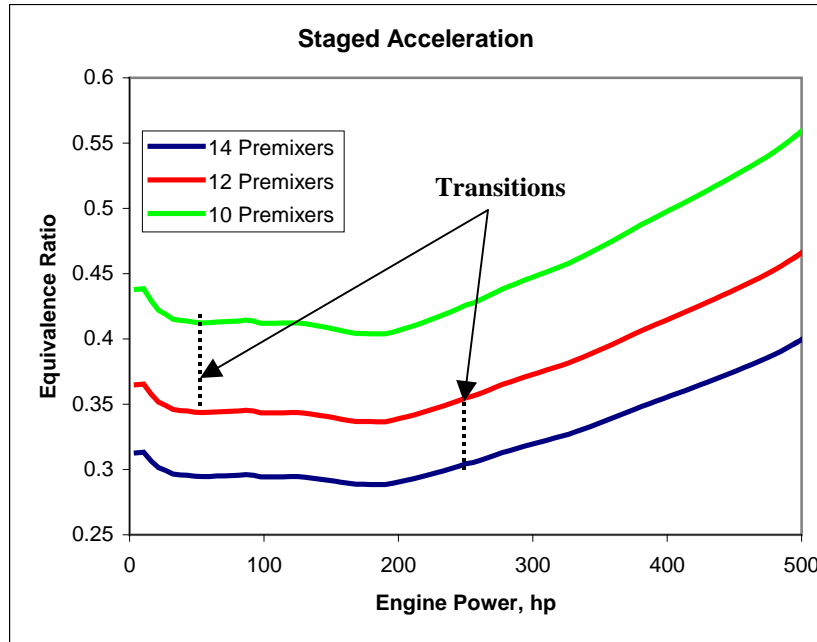


Figure 4.11. Example of staged acceleration.

There are various known methods that could have been used to evaluate the design of the liner to ensure that the premixers were operating at the correct equivalence ratios. One method would be to compare flame temperatures and NO_x levels at known equivalence ratios to the flame temperatures and NO_x levels when testing the premixer with the liner. Because of the direct relationship between equivalence ratio, flame temperature, and NO_x level, these tests could provide a quantitative result to the validation of the design of the combustor liner. However, due to time constraints this project simply used visual inspection to compare the flame characteristics in the test with the liner to the test when the premixer was tested alone at known equivalence ratios. The visual comparisons gave only an estimate as to how well the liner was designed.

The premixer, when tested with the liner section, did experience blowoff at low engine power level conditions. However, this was expected because of the extremely low equivalence ratios produced at these conditions, below 0.3. The premixers demonstrated excellent flashback resistance throughout the majority of the engine operating conditions in the lab. At extremely high power level conditions, around 500 hp, the premixer did experience flashback. Again, during all tests, the combustion instability was present. The instability was identical to the instability observed when testing the premixer without the liner section. The amplitude of the instability was observed to be related to the power level of the test. It can be reasonably assumed

that the instability is directly related to the onset of flashback. This issue was unable to be addressed during the project, but it will be discussed in the Chapter 6.

The overall performance of the liner design can only be accurately measured by the performance of the combustor in the engine. The stability limits and performance of the liner, in conjunction with the premixers, inside the engine will be discussed in Chapter 5.

Chapter 5: Lean Premixed Hydrogen Engine

The Pratt and Whitney PT6A-20 Turbo-prop engine was converted to operate on lean premixed hydrogen. The existing Jet-A combustor was removed and replaced with the new lean premixed hydrogen combustor.

5.1 Engine Set-up

After testing the predicted operating conditions of the engine in the laboratory, the premixers and newly constructed combustion liner were assembled, creating the lean premixed hydrogen-air combustor, shown in Figure 5.1. Each premixer had a type K thermocouple brazed to the outer shell near the exit to detect flashbacks during operation; this can be seen in Figure 5.1. The lean premixed hydrogen combustor was then inserted into the PT6, shown in Figure 5.2. A fuel manifold was built to connect the hydrogen supply to each premixer. Also, a custom-built T4 (combustor exit) thermocouple rake with 8 evenly spaced probes was installed along with the existing T5 (inner turbine) thermocouple rake to monitor internal temperatures. The Thermo Electron Model 42C High Level NO_x Analyzer sampling probe was inserted into the exhaust of the engine. The combustion products were sampled, and NO_x emissions were monitored during engine operation. More details on the engine testing facilities and instrumentation can be found in Villarreal's Thesis.²⁹

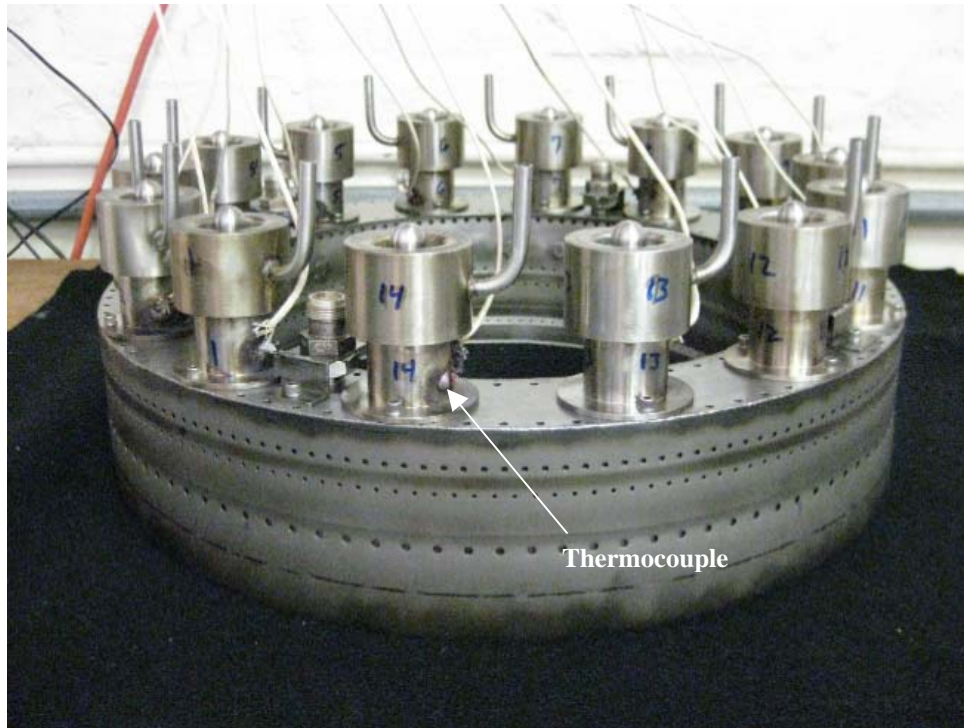


Figure 5.1. Lean premixed hydrogen combustor; consists of 14 hydrogen premixers, a combustor liner, and 4 igniters. Photo by author, 2009.

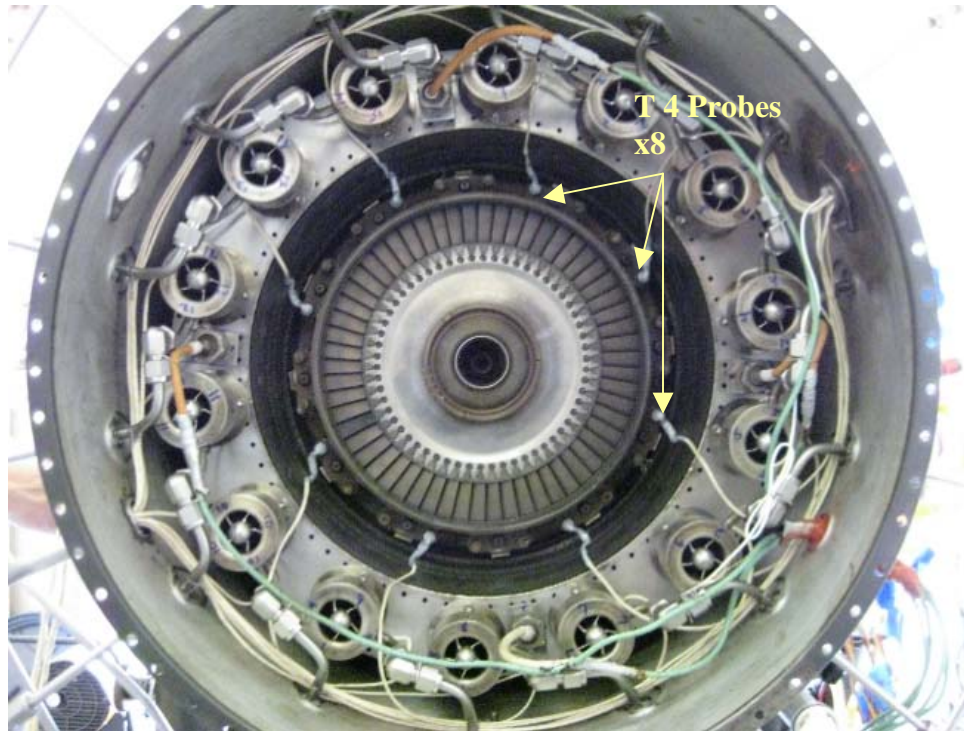


Figure 5.2. PT6A-20 up-fitted with lean premixed hydrogen combustor. Photo by author, 2009.

5.2 Engine Testing and Results

The engine was operated on hydrogen using two different control methods. The first method consisted of a series of manually controlled quarter turn valves and regulators to control the pressure/flow of hydrogen into the engine. The other method used computer controlled solenoids and regulator to automatically control the fuel flow. Both methods continuously monitored engine output power, internal temperatures, and pre-mixer temperatures to guarantee correct behavior. All details on the set-up, equipment, operational procedures, and computer algorithms used to control the engine can be found in Villarreal's Thesis.

Following the procedure given by Villarreal, the engine successfully operated on lean premixed hydrogen through part of the engine's operating range. The inner turbine temperatures were lower than the previous hydrogen designs and were comparable to the original Jet-A configuration. Also, the NO_x levels were in the noise level of the analyzer (below 1 ppm), which was a vast improvement over the original Jet-A configuration and our previous lean premixed hydrogen designs. NO_x data, Figure 5.3, along with T5 temperatures, Figure 5.4, showed that the pre-mixers were stable and operating at or below the design equivalence ratios. The pre-mixers, as expected, had to be brought on in stages; however, it was not as extreme as predicted. All but two of the pre-mixers could be fueled during start-up with the final two pre-mixers coming on at about 50 hp.

The engine successfully operated to 80-85% of the gas generator speed (Ng), which is between 150 and 175 horsepower. The low NO_x levels along with the low internal temperatures confirmed that the design of the combustor liner was working properly. However, the stability of the pre-mixers was worse than predicted. Two pre-mixers suffered flashbacks every time the engine was accelerated above 80-85%.

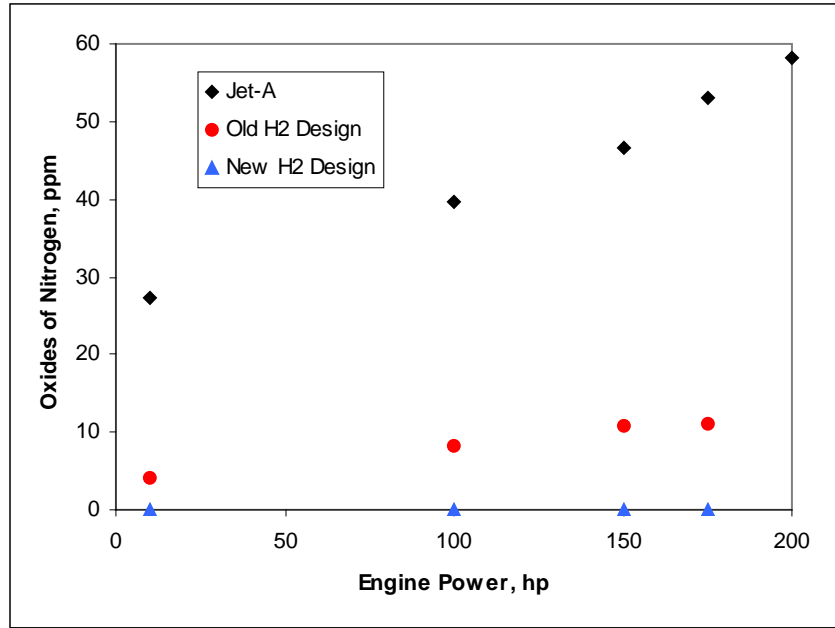


Figure 5.3. Comparison of NOx formation between the original Jet-A engine, the previous iteration of lean premixed hydrogen, and the most recent lean premixed hydrogen combustor design.

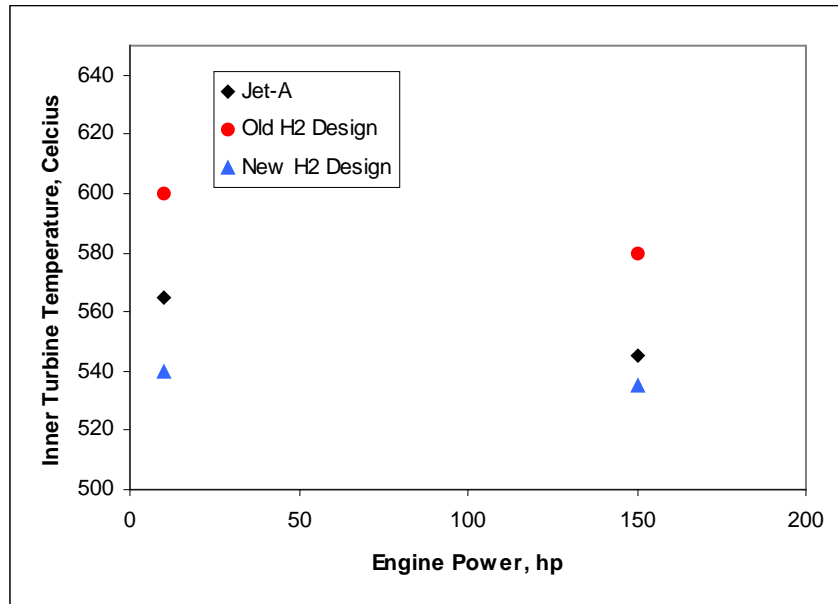


Figure 5.4. Comparison of inner turbine temperatures (T5) between the original Jet-A engine, the previous iteration of lean premixed hydrogen, and the most recent lean premixed hydrogen combustor design.

5.3 Discussion

The implementation of the premixers and the combustor liner went well inside of the engine. The combustor liner along with the 14 premixers fit, as designed, inside of the gas generator case. The only issue with assembling the new combustor in the engine was the design of the fuel delivery manifold. The design was for the fuel tubes to pass through bosses that were located

where the existing Jet-A fuel nozzles went, with no bends. However, after assembling the combustor, the fuel tubes had to be bent to fit onto each premixer. The elbow, fitted to the premixer's fuel tube, extended about 3/8 of an inch too far past where a straight tube could be passed through the gas generator case and fitted to the premixer. Only a slight modification to the premixer would be necessary to make assembly easier in the future.

The combustor liner demonstrated excellent performance when tested in the engine. The low internal temperatures and NO_x emissions measured in the engine during operation confirmed that the premixers were operating at lean equivalence ratios. Even though an exact equivalence ratio could not be measured for each premixer, these observations validated the design methods used to create the combustor liner.

The engine was operated on lean premixed hydrogen using both manual and computer controlled fuel delivery to the engine. Each method proved to be a viable way to accurately control the fuel rate going into the engine. These tests proved that repeatable and reliable operation on hydrogen could be achieved in a gas turbine engine. The engine produced negligible levels of NO_x while maintaining normal internal temperatures. At low power levels, the premixers were turned on in stages to prevent blowoff. However, it was not possible to avoid flashback.

Two premixers suffered flashbacks at around 85% of the gas generator speed. Currently, a few theories have been proposed as to why flashbacks occurred when every other parameter seemed to be correct. One theory suggests that the engine was not providing a uniform flow around the entire combustor. A discontinuity such as a low velocity or a recirculation zone inside of the gas generator case could cause these two premixers to flashback due to low internal velocities. Other theories suggest that because there was a slight increase in combustor pressure loss, the total airflow produced was less than predicted. This was unlikely because there would have been an increase in both NO_x levels and T4 / T5 temperatures due to richer flames, which was not the case. Another theory suggests that the closing of the bleed valve at around this condition created a flow disturbance. The last idea is that the combustion instability observed in the lab is amplified inside of the engine, causing flashback at a much lower power level condition. It had already been confirmed that the instability existed inside of the engine since a high frequency pressure transducer was placed inside of the engine during operation. At the present, it is unclear why the combustor was experiencing flashback. Further work still needs to

be conducted to understand the reasons for flashback inside of the engine at the conditions mentioned above, while not observing them in the laboratory.

One theory that was briefly tested was the idea that the operation of the bleed valve could be creating a disturbance that could somehow lead to a flashback. The theory was formed because the closing of the bleed valve at around 82% Ng coincided with the occurrence of flashbacks. This could still be the case, but some manipulation to the operation of the bleed valve has already been performed with no success. The closing of the bleed valve was incrementally advanced to 77% Ng, yet the flashbacks were still occurring around the same operating conditions. 77% Ng represented the largest deviation from normal operation of the bleed valve before causing the engine to surge.

Chapter 6: Summary and Recommendations for Future Work

This chapter summarizes the findings from this project, noting the major successes and shortcomings. Also presented are ideas that could be used to address the shortcomings and aid in future designs of lean premixed hydrogen combustors for gas turbine engines

6.1 Summary

A lean premixed hydrogen combustor was designed, constructed, up fitted, and successfully operated in a gas turbine engine. It was demonstrated that an existing gas turbine could be converted to operate on hydrogen while maintaining normal internal temperatures, eliminating Carbon, and vastly reducing Nitrogen Oxide emissions. Even though the ultimate goal of operating the engine to full power was not met, many conclusions can be taken from each component of the design. These findings, both good and bad, can be used in the further improvement of this technology to provide clean renewable energy.

The premixer met the majority of the design requirements and showed adequate performance when tested in the laboratory. The premixer concept appeared to be successful in producing a stable hydrogen flame that was sized correctly for the existing engine. However, two factors that need improvement are the mixing and the combustion instability. Incomplete mixing was evident from the CFD model and visual observation of five rich zones during operation. The combustion instability was present in both laboratory and engine experiments. From literature, it is reasonable to conclude that these two problem areas are the ultimate reason for flashbacks in the premixer during engine operation. Table 6.1 shown below shows how the final premixer design performed in comparison to the restrictions and constraints found in section 3.2 Premixer Design.

Table 6.1. Comparison of design parameters for the premixer to the restrictions and constraints placed on the design.

Design Parameter	Restrictions and Constraints	Final Design
Equivalence Ratio (at 500hp)	0.4	0.4
Max Pressure Drop	5%	4%
Internal Velocity	70-100 m/s	70-100m/s
Use of Low Momentum Fuel Jets	Yes	Yes
High Level of Mixing	Yes	No

The combustor liner demonstrated excellent performance characteristics when tested in both the engine and laboratory. The low internal temperatures and NO_x emissions measured in the engine during operation confirm that the premixers were operating at lean equivalence ratios. This performance validated the design methods used to create the combustor liner.

The performance of the engine was a direct result of the operation of the premixers with the combustor liner along with the turbomachinery of the engine. All components worked well at the low to mid power levels of the engine (below 175 hp). However, at higher power levels, the engine ultimately suffered flashbacks. The occurrence of flashbacks during operation could never be avoided or fully understood. The two main theories to explain the flashbacks are that failures in the premixer design are amplified during engine operation or that the engine is producing conditions that were not expected. Due to these shortcomings, much research must be performed to understand the reason for flashbacks and develop methods to eliminate them.

6.2 Recommendations for Future Work

To understand the reason for flashbacks in our current system, work needs to be performed to characterize the environment in which flashbacks are occurring. As mentioned before, laboratory tests under simulated engine conditions failed to produce flashbacks in the premixer, at least until very high power levels. The possible reasons for flashback in the engine that was not seen in the lab need to be investigated; these reasons were already mentioned earlier in this section. To investigate the possibility of a discontinuity in the flow field, a series of static pressure taps should be placed throughout the combustor area during operation of the engine. If a low velocity region was located in the region of the premixer that suffered flashback, measures could be taken to eliminate them. To compare model data to engine data, an apparatus, such as a bell mouth inlet, could be constructed to measure the air flow rate. If discrepancies were found, modifications or a complete redesign of the combustor might be in order to solve the problem.

For future research in this field, it is recommended that the gas turbine selected for modification have a higher pressure drop combustor (above 2%). A gas turbine with higher combustor pressure drops would be less susceptible to flashback because higher internal velocities would be allowable in the premixer design. Higher internal velocities would help to improve the resistance to flashback due to propagation of the flame in the core flow. Also, if all the compressor and turbine maps are known for the engine, it is not necessary to create a model. Knowing the airflow generated by the compressor is crucial for the success of the operation.

It is recommended for future research in this field to investigate the use of pilot fuel capabilities. The use of pilots would allow the premixers to be designed and optimized for a much smaller range of operating conditions. This option could provide the solution to attaining safe and stable operation at full power using a lean premixed hydrogen injector that when in the current configuration would not have been successful.

Studying the engine could prove to be a valuable use of time to understand the reason for flashbacks, but the author believes that a more fundamental understanding of this phenomenon is needed before proceeding to fix the current engine. Currently, there are two major known issues with the premixer: the mixing and combustion instabilities.

The problems with the current mixing have already been discussed in great detail. A redesign of the mixing ports to try to create a more uniform mixture following the same methods discussed before could create more complete mixing. Based on observations, the author suggests using 15 0.020-inch diameter ports evenly spaced at the same injection plane. The author believes the increase in number of evenly spaced ports will greatly improve the level of mixing. Avoiding the wakes, while important, is less important than a uniform mixture. However, this is only because the wakes trailing the vanes in this design quickly diffuse and are not very strong. A more uniform mixture should improve resistance to blowoff and flashback due to the removal of the extremely rich and lean zones.

It is reasonable to assume the main reason for flashback is due to combustion instabilities. From literature, there are four main causes for flashback. The first is flame propagation in the boundary layer, mostly occurring in low speed flows. This is not a major concern in this project because of the extremely thin turbulent boundary layer created by the high-speed flows. Second is flame propagation in the core flow. As discussed in the introduction, the turbulent flame speed is approximated to be around 30 m/s, and the core flow in our premixer is between 70-100m/s. The third cause is combustion induced vortex breakdown. This is unlikely in our design because a centerbody was used to strength and anchor the recirculation zone instead of using a vortex breakdown in the core flow to create the recirculation region to hold the flame zone. It is therefore reasonable to assume that the fourth cause, combustion instabilities, is the main reason for flashback in this design. If the reason the instabilities are occurring can be determined, then it is possible to change the design to eliminate it. The possible reasons could be that certain length scales inside of the premixer are coupling with the acoustic response of the flame, since

combustion instabilities are known to depend heavily on time-lag phenomena.³⁵ It is also possible that the low level of mixing is part of the coupling. Other parameters such as swirl strength or vane design should also be investigated to search for the driving factors causing these instabilities.

A small amount of investigation has already been performed on analyzing the combustion instabilities that were present. Joe Ranalli, a fellow researcher at the time, donated his time and expertise to help capture the frequencies at which the instabilities were occurring, along with some images of the flame during the instabilities. Ranalli used similar techniques that were previously used to conduct research for his dissertation. More details on the techniques used to capture and analyze the data can be found in Ranalli's dissertation.³⁶ The fundamental set-up can be seen in Figure 6.1. The PMT, photo multiplier tube, could be interchanged with the camera to obtain both images of the flame and the total flame intensity. The flow conditions were set to cause the system to go unstable, and the PMT / Camera was focused on the flame to capture the response.

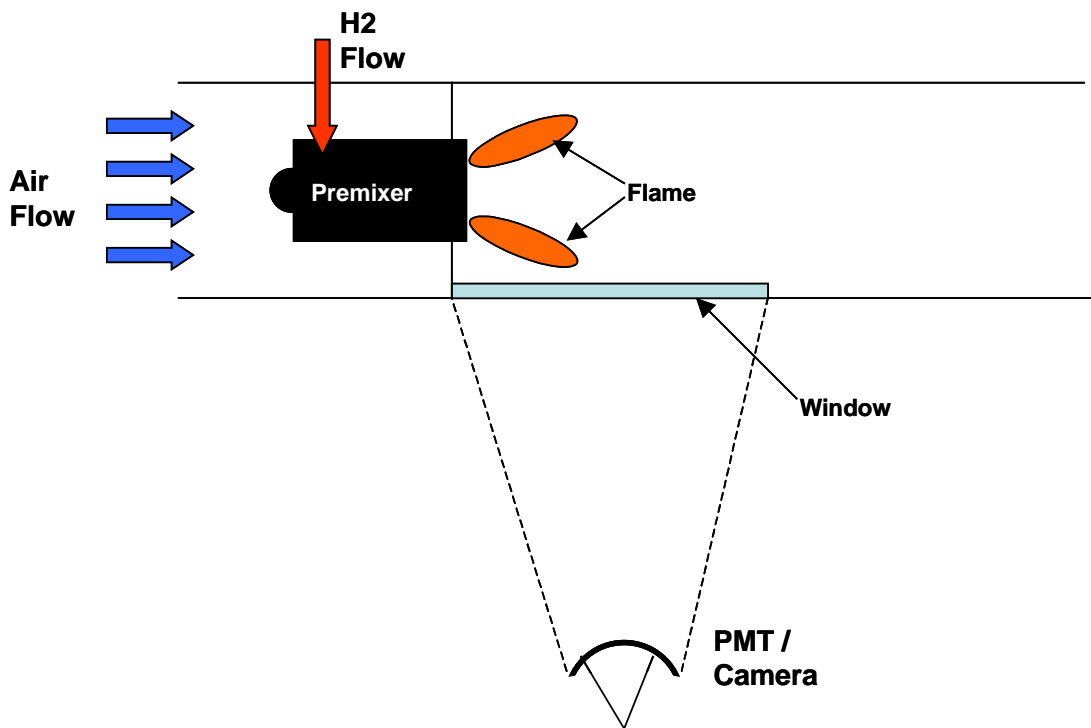


Figure 6.1. Set-up used to capture combustion instabilities.

The PMT was used to record the intensity of the light emitted from the flame during operation. A 308 nm optical bandpass filter was used to collect only the OH* chemiluminescence, a commonly used indicator of flame heat release rate. The intensity was converted to voltage and sampled at 7500Hz for 30 seconds. The power spectrum created from the data is shown in Figure 6.2. The two peaks that appear in the power spectrum, at around 450Hz and 1200Hz, are the frequencies at which the instabilities are occurring.

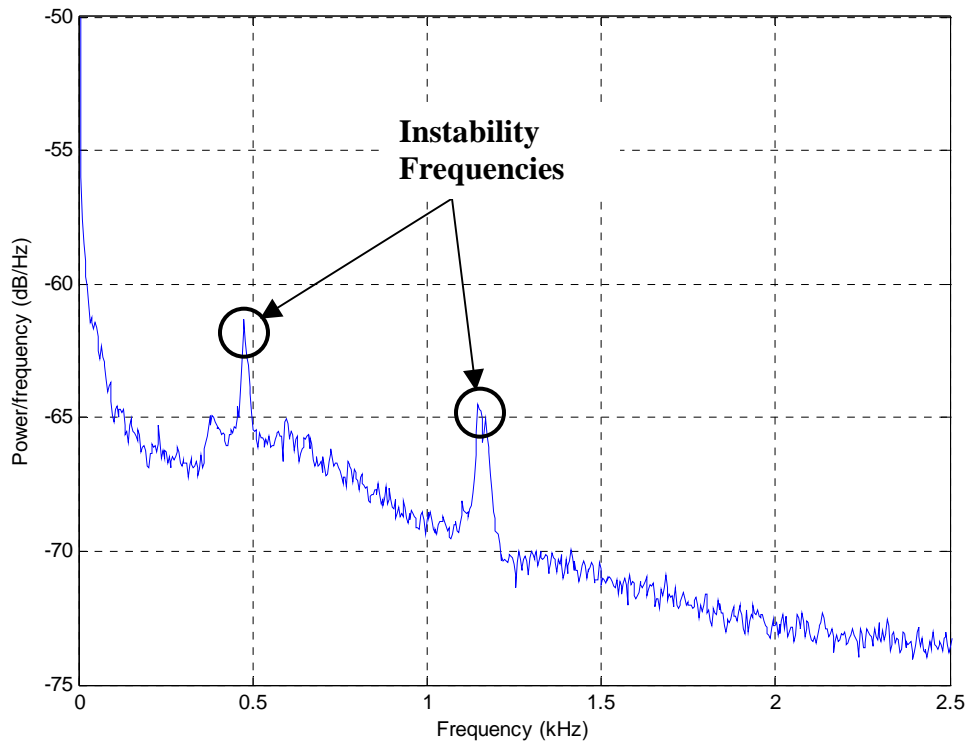


Figure 6.2. Power spectrum for PMT measurements. Peaks at 450Hz and 1200 Hz represent the instabilities.

The camera was used to capture images of the visible flame intensity during the instability. The camera was phase locked to a dynamic pressure sensor and timed to capture a picture of the flame at every 45 degrees of phase. Images were acquired and averaged at each phase for approximately 30 second to reduce fluctuations not caused by the instability, the results of which are shown in Figure 6.3. The images show how the size and shape of the flame fluctuates when the flame is unstable. As mentioned before the fluctuations can become large enough to create conditions in which the flame can propagate upstream causing flashbacks.

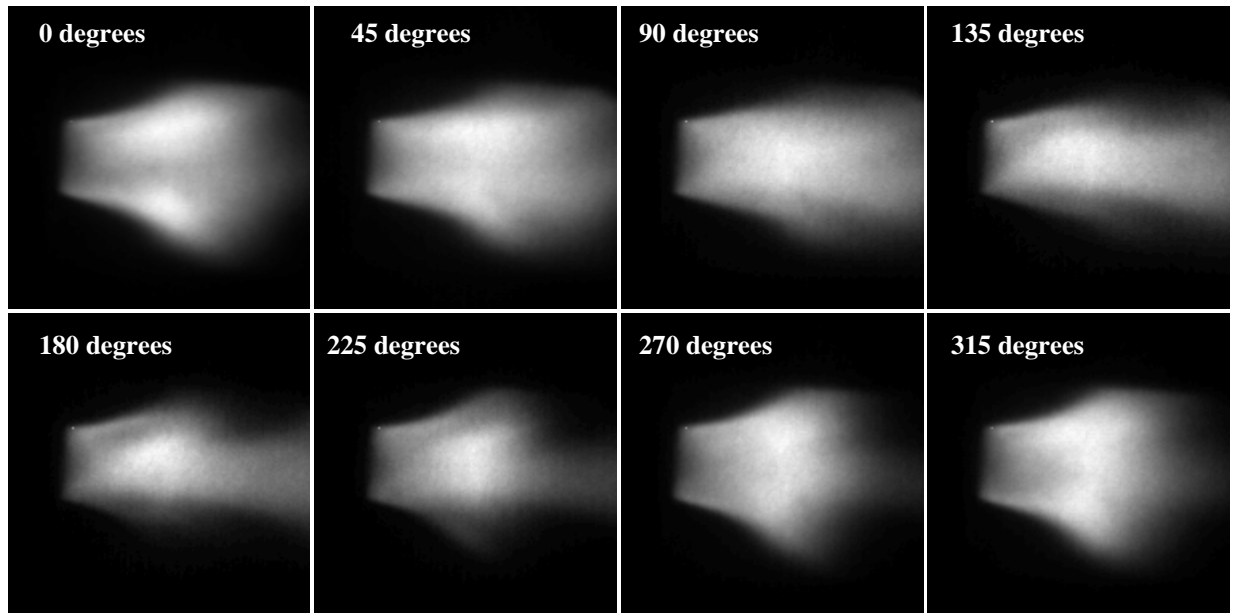


Figure 6.3. Phased averaged images over 1 period. Each picture was averaged at every 45 degrees of phase. Photos by Joe Ranalli, 2009, used with permission.

It is recommended for future work to continue with the research that has already been conducted on characterizing these combustion instabilities. The facilities and experimental techniques already exist to study this topic. Further research could provide insight into the cause of these instabilities, and maybe discover ways to eliminate them. The prevention of combustion instabilities could greatly increase the resistance to flashback in hydrogen premixer designs.

References

- [1] E. I. A. DOE. (2009, June). *Official Energy Statistics from the U.S. Government*. Available: <http://www.eia.doe.gov/>
- [2] G. D. Brewer, *Hydrogen aircraft technology*. Boca Raton: CRC Press, 1991.
- [3] P. Chiesa, G. Lozza, and L. Mazzocchi, "Using hydrogen as gas turbine fuel," *Journal of Engineering for Gas Turbines and Power-Transactions of the Asme*, vol. 127, pp. 73-80, Jan 2005.
- [4] D. M. Wicksall, A. K. Agrawal, R. W. Schefer, and J. O. Keller, "The interaction of flame and flow field in a lean premixed swirl-stabilized combustor operated on H-2/CH4/air," *Proceedings of the Combustion Institute*, vol. 30, pp. 2875-2883, 2005.
- [5] I. Glassman, *Combustion*, 2nd ed. Orlando [Fla.]: Academic Press, 1987.
- [6] S. R. Turns, *An introduction to combustion : concepts and applications*. New York: McGraw-Hill, 1996.
- [7] J. Homitz, "A Lean-Premixed Hydrogen Injector with Vane Driven Swirl for Application in Gas Turbines," M.S., Mechanical Engineering, Virginia Tech, Blacksburg, VA, 2006.
- [8] CHEMKIN, *Computer Modeling of Chemically Reacting Flows*, Sandia National Laboratories, Livermore, CA, 1993
- [9] A. F. Ghoniem, A. Annaswamy, S. Park, and Z. C. Sobhani, "Stability and emissions control using air injection and H-2 addition in premixed combustion," *Proceedings of the Combustion Institute*, vol. 30, pp. 1765-1773, 2005.
- [10] H. S. Guo, G. J. Smallwood, F. S. Liu, Y. G. Ju, and O. L. Gulder, "The effect of hydrogen addition on flammability limit and NOx emission in ultra-lean counterflow CH4/air premixed flames," *Proceedings of the Combustion Institute*, vol. 30, pp. 303-311, 2005.
- [11] G. S. Jackson, R. Sai, J. A. Plaia, C. M. Boggs, and K. T. Kiger, "Influence of H-2 on the response of lean premixed CH4 flames to high strained flows (vol 132, pg 503, 2003)," *Combustion and Flame*, vol. 135, pp. 363-363, Nov 2003.
- [12] G. L. Juste, "Hydrogen injection as additional fuel in gas turbine combustor. Evaluation of effects," *International Journal of Hydrogen Energy*, vol. 31, pp. 2112-2121, Nov 2006.
- [13] R. W. Schefer, "Hydrogen enrichment for improved lean flame stability," *International Journal of Hydrogen Energy*, vol. 28, pp. 1131-1141, Oct 2003.

- [14] O. Tuncer, S. Acharya, and J. H. Uhm, "Dynamics, NO_x and flashback characteristics of confined premixed hydrogen-enriched methane flames," *International Journal of Hydrogen Energy*, vol. 34, pp. 496-506, Jan 2009.
- [15] J. Fritz, M. Kroner, and T. Sattelmayer, "Flashback in a swirl burner with cylindrical premixing zone," *Journal of Engineering for Gas Turbines and Power-Transactions of the Asme*, vol. 126, pp. 276-283, Apr 2004.
- [16] J. O. Keller, L. Vaneveld, D. Korschelt, G. L. Hubbard, A. F. Ghoniem, J. W. Daily, *et al.*, "Mechanism of Instabilities in Turbulent Combustion Leading to Flashback," *Aiaa Journal*, vol. 20, pp. 254-262, 1982.
- [17] S. L. Plee and A. M. Mellor, "Review of Flashback Reported in Pre vaporizing-Premixing Combustors," *Combustion and Flame*, vol. 32, pp. 193-203, 1978.
- [18] B. Lewis and G. Von Elbe, *Combustion, flames, and explosions of gases*, 3rd ed. Orlando: Academic Press, 1987.
- [19] T. Kitagawa, T. Nakahara, K. Maruyama, K. Kado, A. Hayakawa, and S. Kobayashi, "Turbulent burning velocity of hydrogen-air premixed propagating flames at elevated pressures," *International Journal of Hydrogen Energy*, vol. 33, pp. 5842-5849, Oct 2008.
- [20] G. W. Koroll, R. K. Kumar, and E. M. Bowles, "Burning Velocities of Hydrogen-Air Mixtures," *Combustion and Flame*, vol. 94, pp. 330-340, Aug 1993.
- [21] M. V. Perry, "An Investigation of Lean Premixed Hydrogen Combustion in a Gas Turbine Engine," M.S., Mechanical Engineering, Virginia Tech, Blacksburg, VA, 2009.
- [22] A. H. Lefebvre, *Gas turbine combustion*, 2nd ed. Philadelphia: Taylor & Francis, 1999.
- [23] A. K. Gupta, D. G. Lilley, and N. Syred, *Swirl flows*. Tunbridge Wells, Kent: Abacus Press, 1984.
- [24] J. M. Beér and N. A. Chigier, *Combustion aerodynamics*. London,: Applied Science Publishers Ltd, 1972.
- [25] P. G. Hill and C. R. Peterson, *Mechanics and thermodynamics of propulsion*, 2nd ed. Reading, Mass.: Addison-Wesley, 1992.
- [26] S. L. Plee and A. M. Mellor, "Review of Flashback Reported in Pre vaporizing-Premixing Combustors - Reply," *Combustion and Flame*, vol. 37, pp. 335-336, 1980.
- [27] D. Sykes, "Design and Evaluation of a Lean-Premixed Hydrogen Injector with Tangential Entry in a Sector Combustor," M.S., Mechanical Engineering, Virginia Tech, Blacksburg, VA, 2007.

- [28] J. D. Holdeman, "Mixing of Multiple Jets with a Confined Subsonic Cross-Flow," *Progress in Energy and Combustion Science*, vol. 19, pp. 31-70, 1993.
- [29] D. Villarreal, "Digital Fuel Control for a Lean Premixed Hydrogen-Fueled Gas Turbine Engine," M.S., Mechanical Engineering, Virginia Tech, Blacksburg, VA, 2009.
- [30] FLUENT, Flow Modeling Software, Ver. 6.3.26, ANSYS, Canonsburg, PA, 2008
- [31] GSP, Gas Turbine Simulation Program, Ver. 10.0.1.6, NLR, 2009
- [32] Unigraphics, Computer Aided Design, NX-5, Siemens PLM Software, Plano, TX, 2007
- [33] Gambit, CFD Pre-Processor, 2.4.6, Fluent, 2008
- [34] F. P. Incropera and D. P. DeWitt, *Fundamentals of heat and mass transfer*, 5th ed. New York ; Chichester: Wiley, 2002.
- [35] G. A. Richards, D. L. Straub, and E. H. Robey, "Passive control of combustion dynamics in stationary gas turbines," *Journal of Propulsion and Power*, vol. 19, pp. 795-810, Sep-Oct 2003.
- [36] J. A. Ranalli, "Spatially resolved analysis of flame dynamics for the prediction of thermoacoustic combustion instabilities," PhD, Mechanical Engineering, Virginia Tech, Blacksburg, VA, 2009.

Appendix A: Premixer Drawings

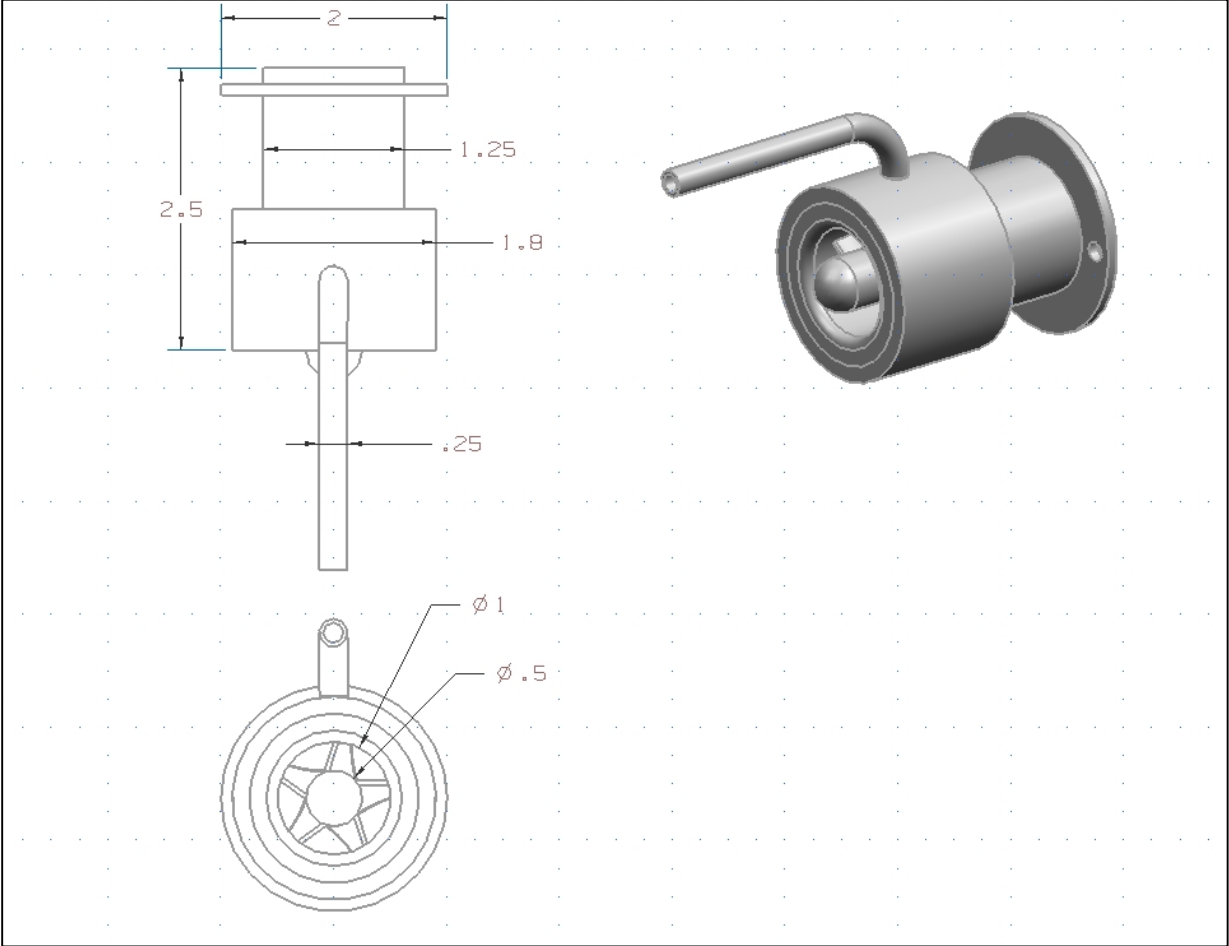


Figure A.1. TOP, FRONT, and ISO view of Premixer

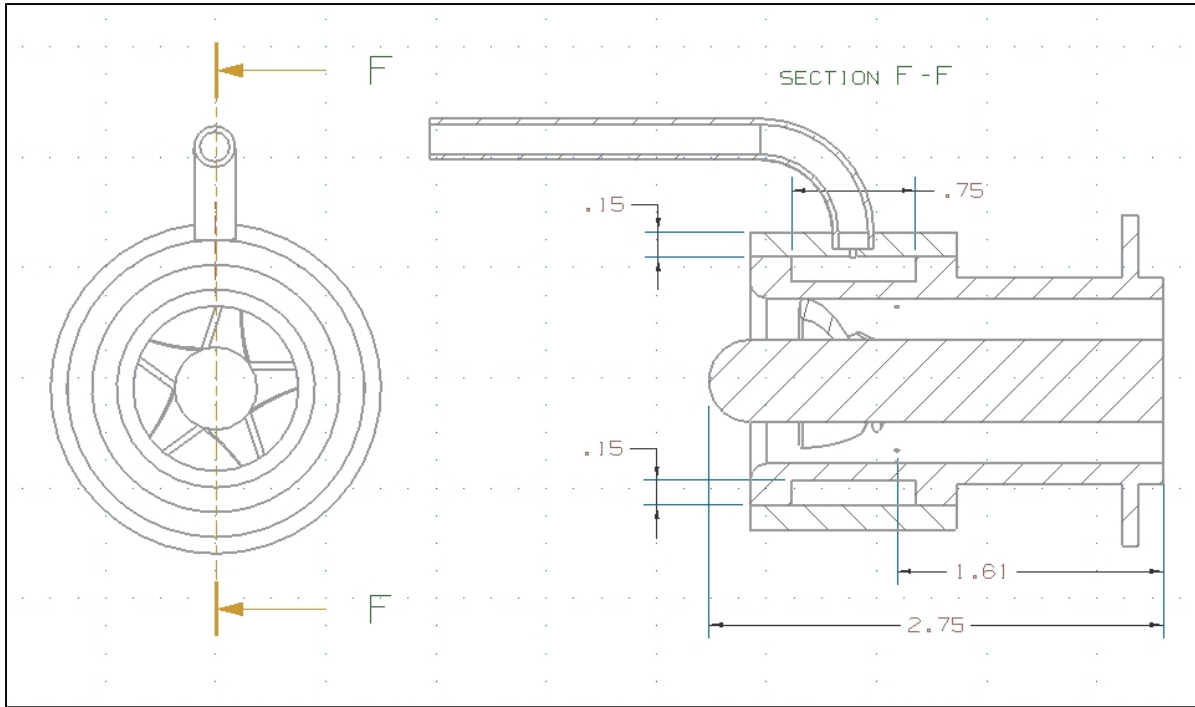


Figure A.2. Section view of Premixer.

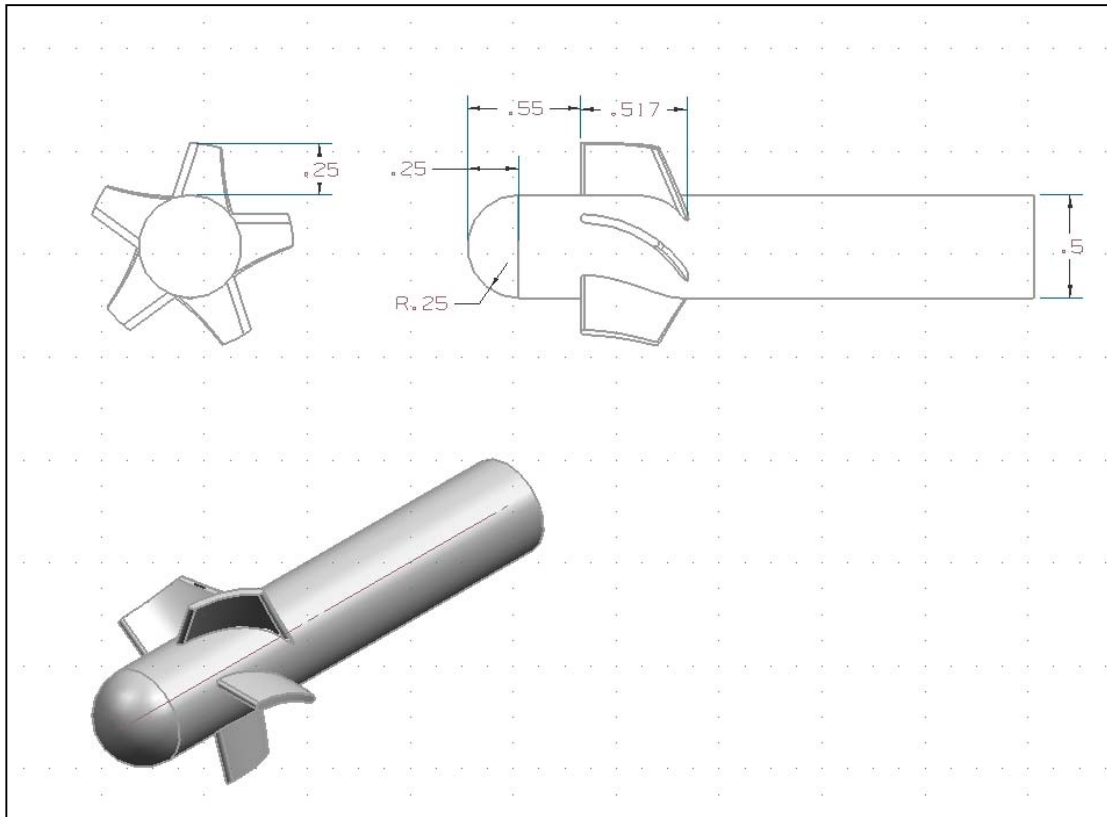


Figure A.3. FRONT, ISO, and RIGHT view of Centerbody

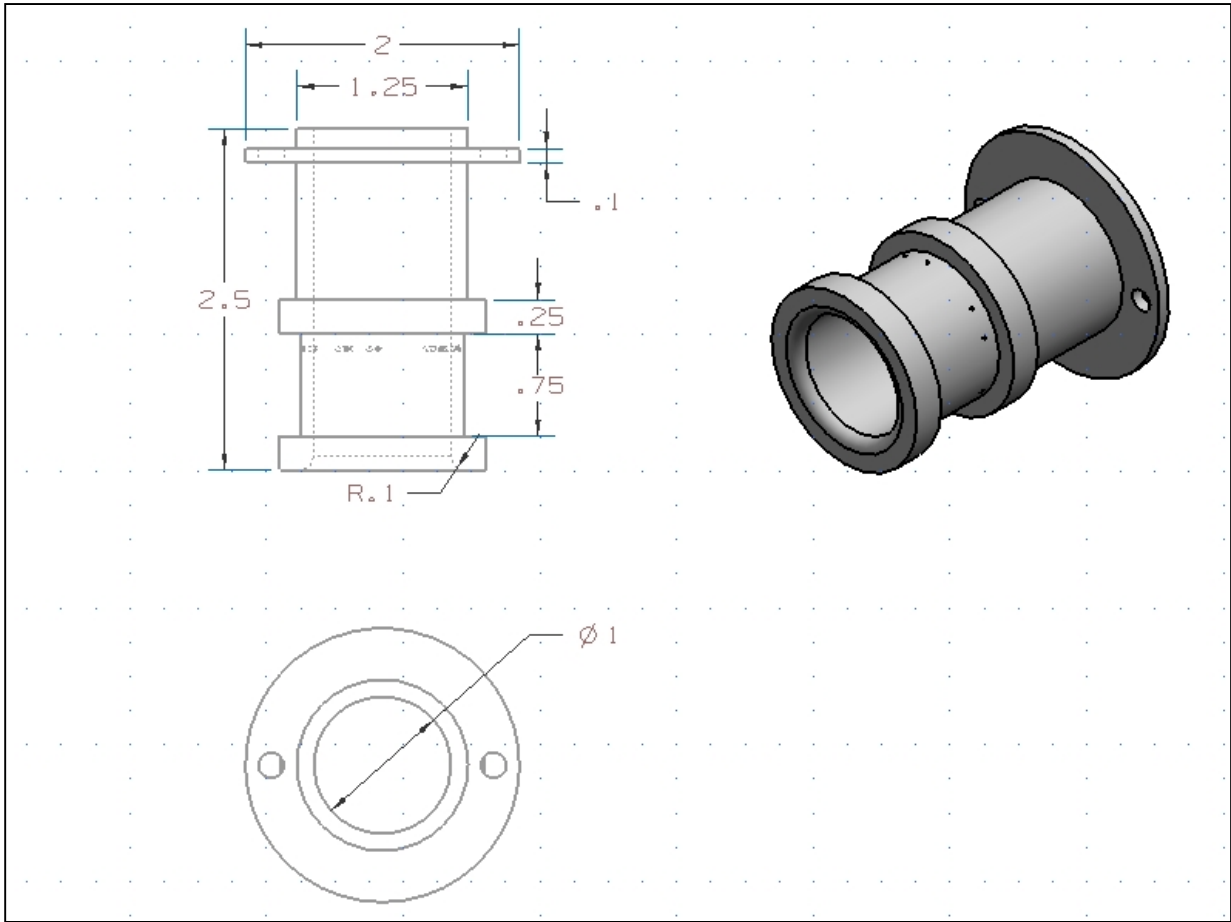


Figure A.4. TOP, FRONT, and ISO view of Premixer Shell

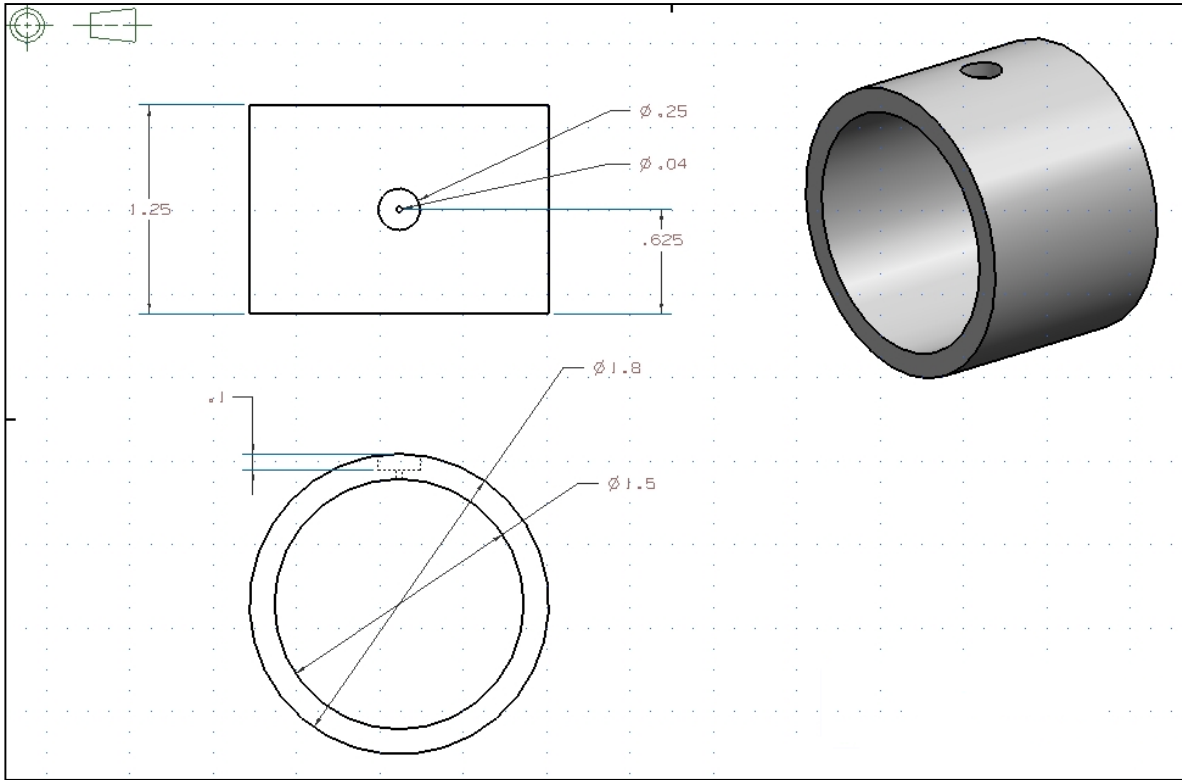


Figure A.5. TOP, FRONT, and ISO view of Fuel Manifold Casing

Appendix B: Computational Model

Table B.1. Settings used for the Computational Model

Computational Fluid Dynamic Model		
Solver		
Solver	Pressure Based	
Space	3ddp	
Formulation	Implicit	
Time	Steady	
Velocity Formulation	Absolute	
Gradient Option	Green-Gauss Node Based	
Porous Formulation	Superficial Velocity	
Viscous		
Model	k-epsilon	
k-epsilon Model	RNG model	
RNG Options	Swirl Dominated Flow	
Near-Wall Treatment	Non-Equilibrium wall Functions	
Cmu	0.0845	
C1-Epsilon	1.42	
C2-Epsilon	1.68	
Swirl Factor	0.07	
Wall Pr Number	0.85	
Species		
Model	Species Transport	
Reactions	None	
Options	Inlet Diffusion	
	Diffusion Energy Source	
Species	Hydrogen	
	Air	
Mixture Properties	Density (kg/m ³)	Ideal Gas
	Cp (j/kg-k)	mixing-law
	k (W/m-K)	0.0454
	Viscosity (kg/m-s)	Ideal-gas-mixing-law
	Mass Diffusivity (m ² /s)	4.10E-05
Solution Controls		
Pressure Velocity Coupling	Simple	
	Under Relaxation Factors	Discretization
Pressure	Varied	Second Order
Density	Varied	Second Order Upwind
Body Forces	Varied	Second Order Upwind
Momentum	Varied	Second Order Upwind
Turbulent Kinetic Energy	Varied	Second Order Upwind
Turbulent Dissipation Rate	Varied	Second Order Upwind
Turbulent Viscosity	Varied	Second Order Upwind
h2	Varied	Second Order Upwind
Energy	Varied	Second Order Upwind

Appendix C: Combustor Drawings

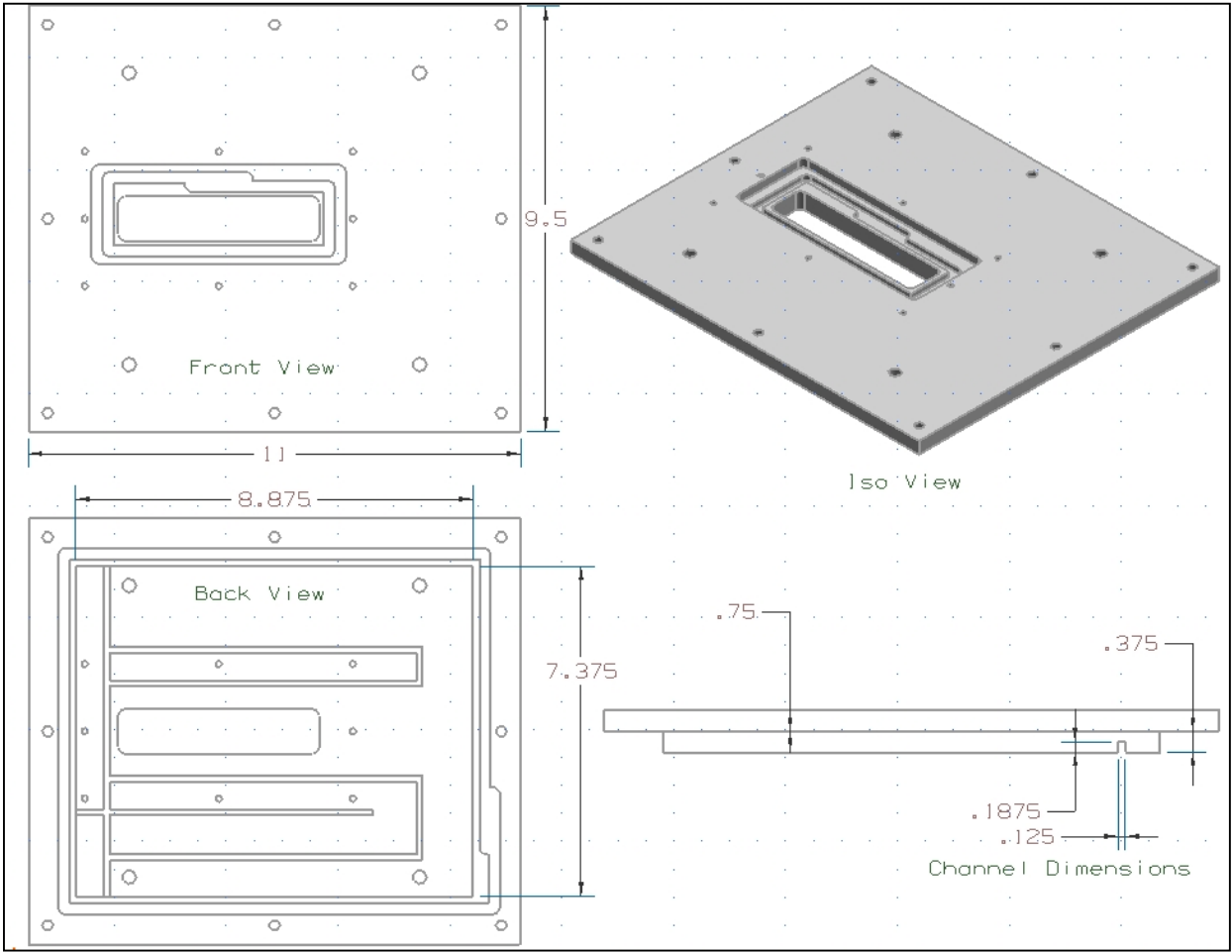


Figure C.1. FRONT, BACK, ISO, and RIGHT view of Front Combustor Plate

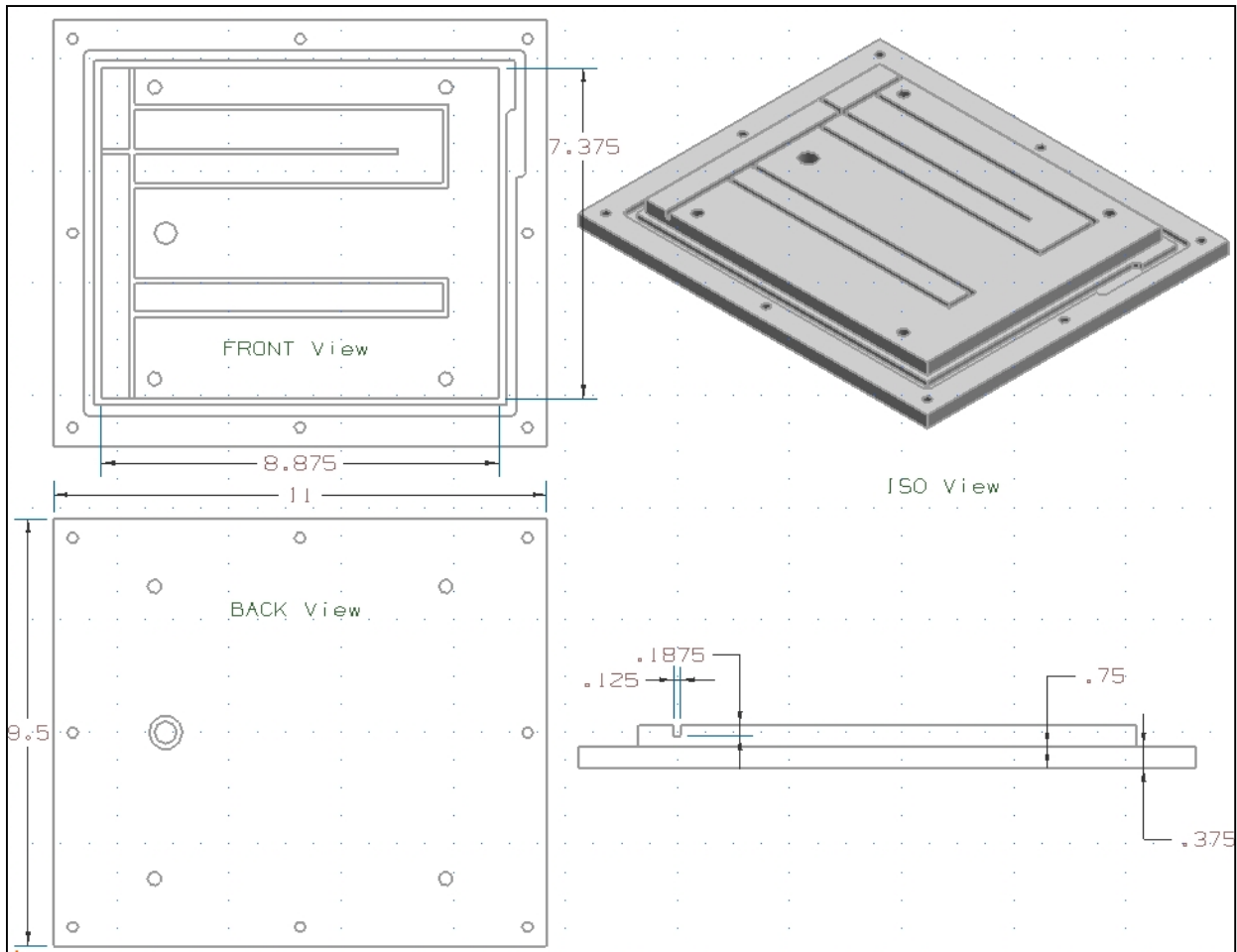


Figure C.2. FRONT, BACK, ISO, and RIGHT view of Back Combustor Plate

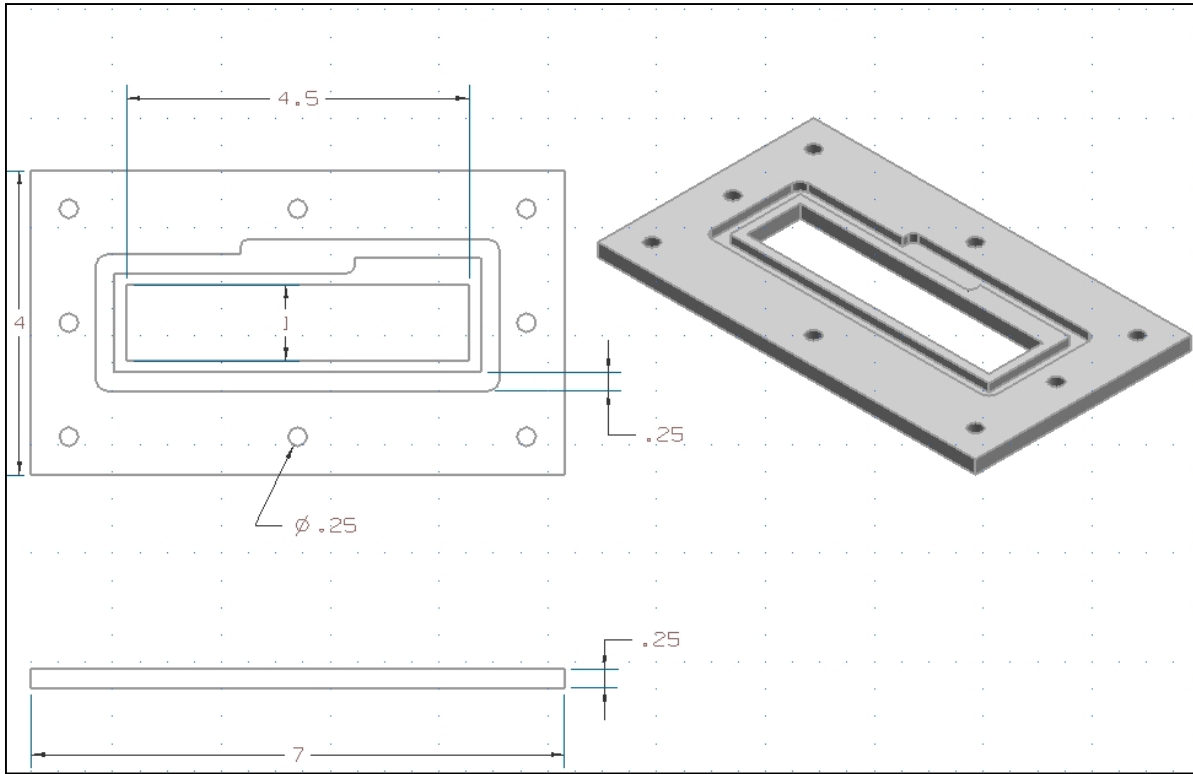


Figure C.3. TOP, FRONT, and ISO view of Combustor Window Cover

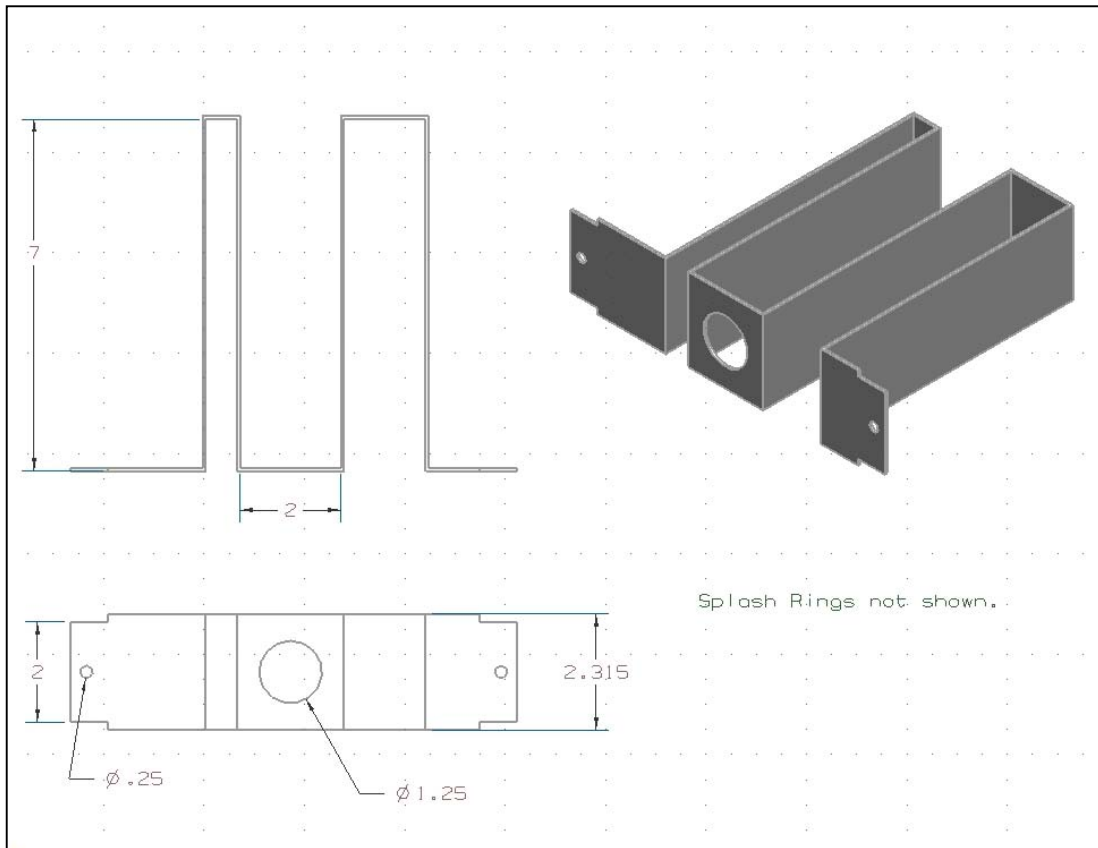


Figure C.4. TOP, FRONT, and ISO view of Liner Section used for Testing.